



**HAL**  
open science

## Implication of actin in the uptake of sucrose and valine in the tap root and leaf of sugar beet

Philippe Michonneau, Pierrette Fleurat-lessard, Anne Cantereau, Alexandre  
Crépin, Gabriel Roblin, Jean-Marc Berjeaud

► **To cite this version:**

Philippe Michonneau, Pierrette Fleurat-lessard, Anne Cantereau, Alexandre Crépin, Gabriel Roblin, et al.. Implication of actin in the uptake of sucrose and valine in the tap root and leaf of sugar beet. *Physiologia Plantarum*, 2021, 172 (1), pp.218-232. 10.1111/ppl.13322 . hal-03119800

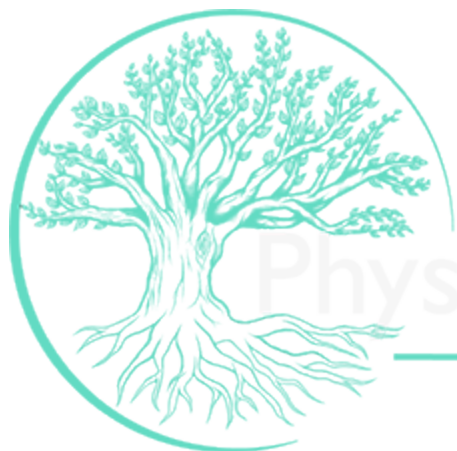
**HAL Id: hal-03119800**

**<https://hal.science/hal-03119800>**

Submitted on 25 Jan 2021

**HAL** is a multi-disciplinary open access archive for the deposit and dissemination of scientific research documents, whether they are published or not. The documents may come from teaching and research institutions in France or abroad, or from public or private research centers.

L'archive ouverte pluridisciplinaire **HAL**, est destinée au dépôt et à la diffusion de documents scientifiques de niveau recherche, publiés ou non, émanant des établissements d'enseignement et de recherche français ou étrangers, des laboratoires publics ou privés.



Physiologia Plantarum

**Implication of Actin in the uptake of sucrose and valine in the tap root and leaf of sugar beet**

Journal:	<i>Physiologia Plantarum</i>
Manuscript ID	Draft
Manuscript Type:	Regular manuscript - Uptake, transport and assimilation
Date Submitted by the Author:	n/a
Complete List of Authors:	Michonneau, Philippe; SCARA Fleurat-Lessard, Pierrette; Universite de Poitiers, Ecologie & Biologie des Interactions, CNRS UMR7267 Cantereau, Anne; Université de Poitiers, STIM, CNRS ERL6187 Crepin, Alexandre; Université de Poitiers, Ecologie & Biologie des Interactions, CNRS UMR7267 Roblin, Gabriel; Universite de Poitiers, Ecologie & Biologie des Interactions, CNRS UMR7267 Berjeaud, Jean-Marc; Universite de Poitiers, Ecologie & Biologie des Interactions, CNRS UMR7267
Key Words:	Beta vulgaris, Cytochalasins, Cytoskeleton, sucrose uptake, valine uptake

1  
2  
3  
4 1 **Implication of Actin in the uptake of sucrose and valine in the tap root**  
5 2 **and leaf of sugar beet**  
6  
7 3  
8  
9

10 4 **Philippe Michonneau<sup>1,2</sup>, Pierrette Fleurat-Lessard<sup>2</sup>, Anne Cantereau<sup>3</sup>, Alexandre**  
11 5 **Crépin<sup>2</sup>, Gabriel Roblin<sup>2</sup>, Jean-Marc Berjeaud<sup>2\*</sup>**  
12  
13 6

14  
15  
16 7 <sup>1</sup> SCARA - Z.I de Villette, 10700 Arcis sur Aube

17  
18 8 <sup>2</sup> Université de Poitiers, Laboratoire EBI (Ecologie et Biologie des Interactions), 1 rue  
19 9 Georges Bonnet, TSA 51106, F-Poitiers Cedex 9, France.

20  
21 10 <sup>3</sup> STIM CNRS 6187, 1 rue Georges Bonnet, TSA 51106, F-Poitiers Cedex 9, France.  
22  
23 11

24  
25 12 \*Corresponding author

26  
27 13 E-mail address: J-M. Berjeaud : jean-marc berjeaud @ univ-poitiers.fr  
28 14  
29 15  
30 16  
31 17

32  
33  
34 18 **Running title:** actin in sucrose and valine uptake  
35

36  
37 19 Number of table: 1  
38

39  
40 20 Number of figures: 9  
41  
42 21  
43  
44  
45  
46  
47  
48  
49  
50  
51  
52  
53  
54  
55  
56  
57  
58  
59  
60

## Abstract

Actin microfilaments (F-actin) are major components of the cytoskeleton essential for many cellular dynamic processes (vesicle trafficking, cytoplasmic streaming, organelle movements). The aim of this study was to examine whether cortical actin microfilaments might be implicated in the regulation of nutrient uptake in root and leaf cells of *Beta vulgaris*. Using antibodies raised against actin and the AtSUC1 sucrose transporter, immunochemical assays demonstrated that the expression of actin and a sucrose transporter, showed different characteristics, when detected on plasma membrane vesicles (PMVs) purified from roots and from leaves. The *in situ* immunolabeling of actin and AtSUC1 sites in PMVs and tissues showed their close proximity to the plasma membrane. Using co-labeling in protoplasts, actin and sucrose transporters were localized along the internal border and in the outermost part of the plasma membrane, respectively. This respective membrane co-localization was confirmed on PMVs and in tissues using transmission electronic microscopy. The possible functional role of actin in sucrose uptake (and valine uptake, comparatively) by PMVs and tissues from roots and leaves was examined using the pharmacological inhibitors, cytochalasin B (CB), cytochalasin D (CD), and phalloidin (PH). CB and CD inhibited the sucrose and valine uptake by root tissues in a concentration-dependent manner above 1  $\mu$ M, whereas PH had no such effect. Comparatively, the toxins inhibited the sucrose and valine uptake in leaf discs to a lesser extent. The inhibition was not due to a hindering of the proton pumping and H<sup>+</sup>-ATPase catalytic activity determined in PMVs incubated in presence of these toxins.

**Key words:** *Beta vulgaris*, cytochalasins, cytoskeleton, sucrose uptake, valine uptake

**Abbreviations:** CB: cytochalasin B; CD: cytochalasin D; PH: phalloidin; PMVs: plasma membrane vesicles

## Introduction

The plant cytoskeleton is generally considered to consist of distinct components, e.g. microtubules, microfilaments and intermediary filaments. The microfilament system has been well characterized in plant cells. In particular, actin microfilaments (MFs or F-actin) are highly organized and major components of the cytoskeleton, and are essential for many cellular processes, including division, expansion, and differentiation (Higaki et al. 2007a, and references therein, Hussey et al. 2006, and references therein). Further, dynamic processes, such as vesicle trafficking, cytoplasmic streaming and organelle movements, are also controlled by MFs (Kantasamy and Meagher 1999, Van Gestel et al. 2002). Moreover, the actin cytoskeleton is implicated in plant defense against pathogens (Hardham et al. 2007, Tian et al. 2009), and MF modification is also observed during elicitor-induced vacuolar disintegration in programmed cell death (Higaki et al. 2007b). Plants express multiple actin isoforms, which are dependent on tissues, organs, and stage of development, suggesting that individual isoforms play specific roles in cells, presumably through interactions with specific actin binding proteins (Kijima et al. 2016). Actin and some of the associated proteins are well conserved in plants and animals (Abu-Abied et al. 2006). The association of actin, in particular, with spectrin (Michaud et al. 1991), myosin (Higaki et al. 2007) and Network (NET) superfamily proteins (Deeks et al. 2012) ensures links with plasma membrane and the association with formin connects cytoskeleton to cell wall (Martinière et al. 2011).

Treatments with pharmacological inhibitors such as cytochalasins and phalloidin (PH) have been widely used to examine the role of actin in the above-mentioned processes, although the mechanism of action of these toxins on actin organization differs. Cytochalasin B (CB) alters the conformation of F-actin microfilaments, whereas cytochalasin D (CD) acts by wedging the polymerization of actin G monomers (Casella et al. 1980), consequently acting more rapidly than CB. Phalloidin (PH) is known to stabilize F-actin filaments by preventing filament depolymerization in response to disruptive agents, including CB (Cooper, 1987). Therefore, PH can be antagonistic to CB on the actin structure located near the plasma membrane, inducing an abnormal accumulation of actin-containing microfilaments.

Based on the multiple effects of MFs on membrane-linked processes, we examine the role of the cytoskeleton in the uptake of metabolites by plant cells. During plant development, photoassimilates are exchanged between sources, suppliers of metabolites (exporting leaves), and sinks importing metabolites (growing and storage organs). Sucrose export from leaf cells is initiated by SWEET-type transporters and is a prerequisite for loading into the companion cells/sieve element complex (Chen, 2014). Cellular sucrose loading is mediated by transporters belonging to the large SUT/SUC family (Lemoine, 2000). In this last case, H<sup>+</sup>-ATPase pumps are necessary to energize nutrient uptake at the plasma membrane by sustaining the proton motive

1  
2  
3 85 force (pmf) (Delrot 1981, Sze 1985, Bush 1990, Serrano 1989, Bouché-Pillon et al. 1994,  
4 86 Lemoine et al. 1996, Vaughn et al. 2002). Numerous studies have focused on nutrient loading in  
5 87 the phloem of leaves (Giaquinta, 1977, Delrot, 1981, Gahrtz et al. 1994, Sauer 2007). Recently,  
6 88 Nieberl et al. (2017) characterized the proton-coupled sucrose symporter BvSUT1, that loads  
7 89 sucrose exclusively into companion cells in source leaves of *Beta vulgaris*. Mechanisms  
8 90 regulating the unloading of nutrients from phloem to sink storage tissues are not yet clearly  
9 91 understood. The transport pathway may be symplastic through plasmodesmata (Esau and Thorsch  
10 92 1985, Van Bel and Kempers 1990, Van Bel and Gamalei 1991, Lucas et al. 1993, Laurel and  
11 93 Lucas 1996) or apo-symplastic. In sugar storage organs, such as beet taproot, a major fraction of  
12 94 sucrose entering the sink cell is directed toward the vacuole through a specific transporter. Jung  
13 95 et al. (2015) identified the sucrose transporter BvTST2.1 in *Beta vulgaris* taproot which imports  
14 96 sucrose into vacuoles coupled to the export of protons.

15 97 The sugar beet is a biennial plant that accumulates nutrients in its taproot during the first year  
16 98 and uses this store in the second year to form reproductive organs. The tap root represents an  
17 99 original structure: its conducting tissues are organized into concentric rings produced by  
18 100 successive supernumerary cambial layers (Lachaud 1964). Nutrients are stored in xylem  
19 101 parenchyma cells, predominantly in the large and outermost phloem parenchyma cells. Their large  
20 102 central vacuole, whose main content is sucrose and water (Leigh et al. 1979), occupies 90% of  
21 103 the cell volume and reduces the cytoplasm to a thin layer with high density. Sucrose accumulation  
22 104 in vacuoles induces a strong osmotic pressure which may vary from 12 to 13 bars from the  
23 105 juvenile to the mature stage in root beet cells (Wyse et al. 1986). Consequently, this pressure is  
24 106 contained in two ways, by increased rigidity of the wall which forms an exoskeleton, and through  
25 107 the support of the cortical skeleton.

26 108 The aim of this study was to examine whether actin microfilaments may be implicated in the  
27 109 regulation of nutrient uptake by plant cells. First, we demonstrated through immunochemical  
28 110 assays the presence of actin and a sucrose transporter in the plasma membrane, and we examined  
29 111 the differences observed in their respective composition in root and leaf tissues. We also  
30 112 characterized their respective membrane localization on plasma membrane vesicles (PMVs) and  
31 113 in tissues using electronic microscopy. Secondly, we examine the effect of CB, CD, and PH on  
32 114 the uptake of sucrose by the root and leaf tissues of sugar beet. Additionally, the activity of these  
33 115 toxins on valine uptake was comparatively examined to determine whether an amino acid  
34 116 transporter also presents comparable physiological responses observed on sucrose transporter.  
35 117  
36 118  
37 119  
38 120  
39 121

## 122 **Materials and methods**

123

### 124 **Plant growth conditions**

125 Sugar beet (*Beta vulgaris* L. cv Aramis) plants were grown at  $20 \pm 1$  °C in a greenhouse on  
126 vermiculite under natural **day-night** conditions. Supplementary lighting was provided with  
127 OSRAM 58/10 fluorescent tubes, giving a fluence rate of  $80 \mu\text{mol photon m}^{-2} \text{s}^{-1}$  from 6.00-9.00  
128 a.m. and from 7.00-10.00 p.m. Relative humidity was maintained at  $60 \pm 10\%$ . The plants were  
129 watered daily with [Snyder and Carlson \(1978\)](#) nutritive solution. **Plants were used for experiments**  
130 **when they were 4 months old, bore seven mature expanded leaves and had root diameter of**  
131 **approximately 2 cm (Fig. 1 A).**

### 132 **Transport assays *in vivo***

133 The assays on taproot tissues were carried out as previously described ([Michonneau et al., 2004](#)).  
134 Tissue cylinders of 12 mm diameter were taken from the root cortex using a cork borer. These  
135 cylinders were sliced into discs of 1 mm thickness and  $0.1100 \text{ g} \pm 0.0013 \text{ g}$  mass and subsequently  
136 divided into four quarters of  $0.0268 \text{ g} \pm 0.0030 \text{ g}$ , to facilitate the uptake of the substrates. The  
137 quarters were immersed in a basal medium (BM) containing 300 mM sorbitol, 0.5 mM  $\text{CaCl}_2$ ,  
138 0.25 mM  $\text{MgCl}_2$ , 20 mM MES (pH 5.4).

139 Leaf discs (80, 6 mm diameter each) were excised after peeling off the lower epidermis and  
140 incubated (peeled face downwards) on BM. Harvesting was carried out in areas containing only  
141 minor veins.

142 Radiolabeling studies were carried out on root tissue quarters and leaf discs in BM containing  
143 1 mM [ $^{14}\text{C}$ ] sucrose (final activity  $11 \text{ kBq ml}^{-1}$ ) and 1 mM [ $^3\text{H}$ ] valine (final activity  $9.25 \text{ kBq ml}^{-1}$ ).  
144 Incubation was run for 30 min under mild agitation on a shaker at 25°C. At the end of the  
145 incubation, the root quarters were rinsed (3 x 3 min) in BM and were placed in scintillation **vials**.  
146 **Solubilization of the tissues occurred at 55°C during 24 h in a mixture of perchloric acid (56%),**  
147 **0.1%  $\text{H}_2\text{O}_2$  (27%), and Triton X-100 (17%).** Discs of exporting leaves were treated in the same  
148 way except that the mixture used for **solubilization consisted of** perchloric acid (25%),  $\text{H}_2\text{O}_2$   
149 (50%) and Triton X-100 (25%). Finally, 4 ml of scintillation liquid (Ecolite™, ICN) was added  
150 to the tubes and radioactivity was counted by liquid scintillation spectroscopy (1900 TR Packard).

### 151 **Preparation of protoplasts**

152 Protoplasts were prepared from the taproot and leaf blade according to [Fleurat-Lessard et al.](#)  
153 [\(1993\)](#). Tiny slices of root tissues and peeled leaf discs were stored in the predigestion medium  
154 (0.6 M mannitol, 25 mM MES, 8 mM  $\text{CaCl}_2$  and 2 mM  $\text{MgCl}_2$  at pH 5.6) for 1 h at 28°C to be

1  
2  
3 155 **plasmolyzed**. Digestion occurred in the dark for 2h at 30°C in the same medium, supplemented  
4 with 1.5% pectolyase (Seishin Pharmaceutical Co., LTD, Tokyo, Japan), 2% macerozyme R-10  
5 156 and 3% cellulase (Yakult, Pharmaceutical Industry Co., Ltd, Nishinomiya, Japan). Then,  
6 157 protoplasts (60 to 80 µm in width) were isolated at 4°C on a Ficoll gradient by a 30 min  
7 158 centrifugation at 900 g.  
8 159

### 160 **Isolation and uses of plasma membrane vesicles from root and leaf tissues**

161 Purified PMVs were prepared by phase partitioning of microsomal fractions from the leaf and  
162 root tissues of sugar beet according to Lemoine et al. (1991) with some minor modifications.  
163 The PMVs at a concentration of 15 µg ml<sup>-1</sup> were equilibrated in a medium containing 0.3 mM  
164 sorbitol, 50 mM potassium phosphate (pH 7.5), 0.5 mM CaCl<sub>2</sub>, 0.25 mM MgCl<sub>2</sub>, and 0.5 mM  
165 DTT, frozen in liquid nitrogen and stored at -80 °C. The PMVs were placed in the inside-out  
166 configuration by adding 0.05% Brij in the assay medium. In the four batches of vesicles used in  
167 this work, treatment with the plasma membrane H<sup>+</sup>-ATPase inhibitor sodium orthovanadate at  
168 0.25 mM (Gallagher and Leonard, 1982; O'Neill and Spanswick, 1984) showed that 75% of the  
169 enzyme activity can be attributed to plasma membrane functioning. Vanadate-sensitive ATPase  
170 activity of the PMVs was measured in a medium buffered with 50 mM tris-maleate at a pH  
171 of 6.9 (Noubhahni et al., 1996). Proton pumping was measured by the decrease of 9-  
172 aminoacridine absorbance at 495 nm in a medium buffered with 10 mM tris-maleate at a pH of  
173 6.9 (Noubhahni et al., 1996). The reaction was initiated by the addition of 3 mM MgSO<sub>4</sub> to the  
174 medium. Protein content was measured using the method of Bearden (1978).

175 When measuring the uptake of sucrose and valine, PMVs were placed in an  
176 “energized” state following resuspension in 50 mM sodium phosphate (pH 5.5),  
177 containing 10 µM valinomycin (condition creating pH and Ψ gradients) (Lemoine et al.,  
178 1991). Uptake assays were carried out as previously described (Michonneau et al., 2004).  
179 Briefly, uptake was initiated by rapidly mixing vesicles with the incubation medium  
180 containing 1 mM [U-<sup>14</sup>C]sucrose (final activity: 27 kBq ml<sup>-1</sup>) and 1 mM [<sup>3</sup>H]valine (final  
181 activity: 41 kBq ml<sup>-1</sup>). Uptake was stopped after 3 min by adding 2 ml medium containing  
182 5 mM HgCl<sub>2</sub>. The content of the test tubes was filtered using Millipore HAWP filters  
183 (pore size 0.45 µm). The filters were then rinsed, placed in a scintillation vial, dried at 50  
184 °C for 1 h, and immersed in 4 ml of scintillation liquid for counting. **In the dedicated**  
185 **experiments, inhibitors (Vanadate, CB, CD, PH) were added to the PMV incubation**  
186 **medium, 30 min before determining H<sup>+</sup>-ATPase activity and uptake of sucrose and valine.**

### 187 **Electrophoresis and immunological assays**

188

1  
2  
3 189 SDS-PAGE was performed according to Laemmli (1970) using 10 % polyacrylamide, 0.21%  
4 190 bisacrylamine gels. The gels were run at room temperature under a constant current of 15 mA.  
5 191 The gels which were equilibrated in 25 mM tris, 192 mM glycine and 20% methanol at a pH of  
6 192 9.4, were electrotransferred onto nitrocellulose (Towbin et al., 1979) for 1 h at 200 mA. After the  
7 193 saturation of the non-specific sites, incubation with the primary antibody was performed in  
8 194 phosphate buffer saline (PBS) plus 0.1 % BSA for 90 min at 10 °C. A anti-actin antibodies raised  
9 195 in mice (ICN, 691002, titer 1 mg ml<sup>-1</sup>) were used. Anti-AtSUC1 antibodies raised in rabbit (a kind  
10 196 gift from Professor Ruth Stadler, University of Erlangen, Germany) against the sucrose carrier 1  
11 197 of *Arabidopsis thaliana* as described by Sauer and Stolz (1994) has been successfully  
12 198 experimented on sugar beet by Sakr et al. (1997). Interestingly, the expression of *AtSUC1* was  
13 199 observed in many tissues (Feuerstein et al. 2010), particularly in roots (Sivitz et al. 2008). After  
14 200 rinsing, the secondary antibody, GAM-peroxidase for actin and GAR-peroxidase for AtSUC1  
15 201 (Biorad, Marnes la Coquette, France), diluted at 1/2000 in the saturation medium was used. The  
16 202 antigen-antibody complex was examined using the kit ECL RPN 2106 (GE Healthcare Europe  
17 203 GmbH) which contained the substrate of the conjugate peroxidase. The subsequent light emission  
18 204 was monitored on film (Hyperfilm, GE Healthcare Europe GmbH) treated with 1/10 Ilford Ilfotec  
19 205 LC 29 and 1/10 Ilford Rapid Fixer. The positions of the bands were compared with the molecular  
20 206 weight of prestained standards (SeeBlue<sup>R</sup> Plus2, Invitrogen).

31 207

### 32 208 **Microscopy and *in situ* immunolocalization**

33 209 Protoplasts isolated from the taproot and leaf blade were examined with a spectral confocal station  
34 210 FV1000 which was installed on an inverted microscope IX-81 (Olympus, Tokyo, Japan). Double  
35 211 fluorescence images were acquired sequentially with an Olympus UplanFLN x 40 oil, 1.3 NA  
36 212 objective lens. Green fluorescence was excited with the 488 nm line of an argon laser and the  
37 213 emitted fluorescence was detected through a spectral detection channel between 500 and 530 nm.  
38 214 Red fluorescence was obtained sequentially with a 543 nm line of a HeNe laser and detected  
39 215 through a channel between 555 and 655 nm. Images were maximum intensity projections which  
40 216 resulted from the optical sectioning of the specimen (20-60 sections, 1 µm step). The localization  
41 217 of actin and AtSUC1 in protoplasts was obtained by applying the antibodies either separately or  
42 218 simultaneously to achieve a co-localization of both components. F-actin was identified via the  
43 219 tetramethylrhodamine isothiocyanate (TRITC)-phalloidin probe that emits red fluorescence and  
44 220 AtSUC1 via the fluorescein isothiocyanate (FITC) probe that emits green fluorescence.

45 221 For transmission electron microscopy (TEM), the samples of plant tissues were treated as  
46 222 previously described (Bouché-Pillon et al. 1994; Fleurat-Lessard et al. 1997). Briefly, samples  
47 223 were fixed for 45 min at 4°C in 2% paraformaldehyde/0.5% glutaraldehyde (w/v) prepared in  
48 224 Sørensen buffer at pH of 7.4, washed extensively in the buffer containing 7.5% sucrose, postfixed

60

1  
2  
3 225 in 1% (v/v) osmium tetroxide, dehydrated in an increasing ethanol series, and embedded in  
4 226 London Resin White (LRW) by polymerization conducted at 60°C for 24 h. Ultrathin sections  
5 227 (70 nm thick) of these chemically fixed samples were collected on gold grids and immunotreated.  
6 228 Briefly, the samples on the grids were rehydrated and treated with 0.5 M NaIO<sub>4</sub> for 25 min and  
7 229 0.1 M HCl for 8 min to expose the antigen sites. The non-specific sites were saturated by the  
8 230 addition of 10 mM PBS (pH 7.2), 0.1% Triton X-100, 0.2% Tween 20, 0.1% BSA and 1/20 normal  
9 231 goat serum (NGS, Nordic, TEBU, Le Perray en Yvelines, France) for three times for 5 min each).  
10 232 The primary antibody (see western blot analyses) was diluted at 1/50 in the saturation medium  
11 233 and added to the samples followed by overnight incubation at 4°C. The grids were then saturated  
12 234 using Tris-buffered saline (TBS) (pH 8.2), 0.1% Triton X-100, 0.2% Tween 20, 0.1% BSA, 1/20  
13 235 NGS for 1 h. The secondary antibody coupled to gold particles (15 nm size) (EM GAR 15 nm,  
14 236 Biocell, TEBU) was applied to the TBS solution for 3 h.

15 237 Immunolabellings of actin and AtSUC1 were done on ultrathin sections which were obtained  
16 238 from the tissues and on purified fractions of PMVs which were isolated from roots and leaves.  
17 239 They were fixed and embedded as described above. Anti-actin and anti-AtSUC1 were added to  
18 240 the saturation medium at a 1/30 dilution. The co-localization of actin and AtSUC1 was achieved  
19 241 using 1/50 diluted secondary antibodies which were applied together and labeled with gold  
20 242 particles of different sizes, including 5 nm for actin (EM GAM 5 nm, Biocell, TEBU) and 10 nm  
21 243 for AtSUC1 (EM GAR 10 nm, Biocell, TEBU). After washing in TBS (three times for 15 min)  
22 244 and distilled water for 15 min, the samples on the grids were contrasted and observed in TEM  
23 245 using a JEM 1010 Jeol microscope operating at 80 kV.

24 246 Three independent immunoassays were performed. Counting was made using pictures  
25 247 obtained from six samples of PMVs and tissues from the leaves and roots. Five to eight pictures  
26 248 from each sample were analyzed. Controls were obtained by omitting the primary antibody from  
27 249 the experiment.

28 250

## 29 251 **Chemicals**

30 252 Stock solutions of the effectors were prepared as follows: CB at 0.240 mg ml<sup>-1</sup> (500 μM) in  
31 253 distilled water containing ethanol (30%), CD at 5 mg ml<sup>-1</sup> (10 mM) prepared in pure DMSO and  
32 254 PH at 7.90 mg ml<sup>-1</sup> (10 mM) was dissolved in 100% ethanol. Control tissues were treated at the  
33 255 maximum by 0.6% ethanol or 0.1% DMSO.

34  
35  
36  
37  
38  
39  
40  
41  
42  
43  
44  
45  
46  
47  
48  
49  
50  
51  
52  
53  
54  
55  
56  
57  
58  
59  
60

## 257 **Results**

### 258 **Anatomical and cytological characteristics of the root and leaf tissues**

259 During the development of the *Beta* root, cambium produced the secondary phloem and xylem.  
260 These secondary structures expanded considerably because of the increase in the number and  
261 width of pericycle and associated vascular cells distributed in concentric layers. At the harvesting  
262 stage, the differentiation of supernumerary cambium has led to the formation of six or seven  
263 concentric layers of vascular tissues which were separated by large pericycle areas as shown in  
264 the autoradiographic images obtained after treatment with [<sup>14</sup>C]sucrose (**Fig. 1B**). From this  
265 image, one can deduce that the vascular tissue layer (composed of conducting elements  
266 surrounded by parenchyma in vascular bundles and by interfascicular parenchyma) was about  
267 one-third the thickness of the storage pericycle layer (**Fig. 1C**). Storage pericycle cells (60-70 μm  
268 wide) were characterized by a large central vacuole that flattened the thin cytoplasm and the  
269 nucleus against the pectocellulosic wall (thicker than the cytoplasm) (**Fig. 1D, D'**).

270 In the leaf discs, [<sup>14</sup>C]sucrose labeling was observed mainly in the veins and mesophyll cells  
271 (**Fig. 1E**). The determination of the respective areas from this cross-sectioned image indicated  
272 that mesophyll cells occupied half of the total area. Cross sections of a small leaf vein  
273 (approximately 60 μm wide) showed that xylem and phloem tissues, which were surrounded by  
274 the bundle sheath, were surrounded by several layers of large mesophyll cells (each at least 60  
275 μm wide and 100 μm long) (**Fig. 1F**). The mesophyll cells contained large vacuoles and several  
276 plastids with starch grains and wide nuclei (**Fig. 1G**). Additionally, the cytoplasm of the leaf cells  
277 was thicker than that of the root cells.

### 278 **Co-localization of actin and a putative sucrose carrier in storage root cells and in** 279 **mesophyll cells of sugar beet**

280 As shown by the western blot analysis of the PMVs (**Fig. 2**), using an antibody raised against  
281 actin, labeled actin was localized at 42 kDa on protein extracts of roots and leaves. The quantity  
282 of actin was in lower amounts in the leaf extracts than the root extracts. The anti-AtSUC1  
283 antibody, raised against the sucrose transporter SUC1 from *Arabidopsis* was chosen because of  
284 its high expression as well in leaves as in roots (Sivitz et al. 2008). It labeled three protein bands  
285 in root extracts (two main bands at 42 and 56 kDa and a band of low intensity at 46 kDa) and a  
286 distinct band in leaf extracts at 42 kDa.

287 However, to examine the possible structure and function link, the involved element must be  
288 localized in an appropriate place in the cell. To address this issue, subcellular localization was  
289 carried out on the PMVs isolated from the root and leaf tissues. An immunogold labeling detected  
290 on PMVs purified from roots and leaves, using antibodies raised against actin (**Fig. 3A, D**) and

the sucrose transporter AtSUC1 (Fig. 3B, E) compared with the control treatment (Fig. 3C, F) specified the localization of both proteins in the purified membrane fraction. As shown in ultrathin sections of the storage root cells (Fig. 4A, B, C) and of leaf parenchyma cells (Fig. 4D, E, F), labeling with gold particles confirmed the subcellular localization of both components. The labeling of the sucrose carrier appeared to be localized in the outer region of the membrane compared with the labeling of actin which was localized in the internal region. It is important to emphasize that no labeling was observed on the vacuolar membrane.

The *in situ* immunolocalization revealed that labeled actin and sucrose carriers were detected in the cortical area of the protoplasts of the root storage cells (Fig. 5A, B, C, D, E) and mesophyll cells (Fig. 5F, G, H, I, J). However, the sucrose carrier appeared to be localized externally compared with the actin in both types of protoplasts (Fig. 5D, I). Furthermore, the immunolabeling observed in electron microscopy, using gold-labeled secondary antibodies which were applied simultaneously (EM GAR 10 nm for sucrose transporter and EM GAM 5 nm for actin), allowed the determination of the distance separating the two sites. The distance measured between the large and small gold particles was  $44 \pm 3$  nm (mean  $\pm$  SE;  $n = 30$ ) in the PMVs from the roots (Fig. 6A) and  $48 \pm 4$  nm ( $n = 30$ ) in the PMVs from the leaves (Fig. 6B). In tissues, the distance was  $45 \pm 4$  nm ( $n = 42$ ) in the root cells (Fig. 6D) and  $44 \pm 2$  nm ( $n = 48$ ) in the mesophyll cells (Fig. 6E). However, Student Fisher *t* test showed that the differences were not statistically significant at 5% confidence level. Gold labeling was absent in controls obtained after primary antibody omission, as shown in the PMVs (Fig. 6C). In addition, it should be stressed that the co-localization indicated that labeled sites were not located in definite microdomains.

### Effect of cytochalasin B, cytochalasin D, and phalloidin on sucrose and valine uptake by beet tissues

To determine whether actin may be functionally implicated in the activity of transporters, we tested known inhibitors of actin microfilament arrangement, namely CB, CD and PH.

In line with previously reported data (Michonneau et al., 2004) the capacity of sucrose uptake by the root tissues increased continuously and considerably until 12 h of aging in the control samples (Fig. 7A). This phenomenon has been largely investigated in leaf tissues (Sakr et al., 1993; 1997) (Fig. 7B). After this period, a significant decrease in net sucrose uptake was observed, particularly in the root tissues. CB, CD and PH did not control the sucrose uptake in the roots and in leaves with the same intensity (Fig. 7A, B). Additionally, increasing the treatment duration from 3 to 6, 12, and 24 h increased the inhibition of net sucrose uptake in the roots from 5 to 20, 37 and 57% for CB and from 0 to 17, 24 and 34% for CD, respectively (Fig. 7A). Additionally, during increase in treatment duration from 3 to 6, 12, and 24 h, 10  $\mu$ M CB inhibited

uptake in the leaves from 8, 18, 18, and 5%, while 10  $\mu\text{M}$  CD inhibited uptake from 7 to 14, 7 and 10% (**Fig. 7B**). Sucrose uptake was significantly inhibited in the roots and leaves after 6 h treatment with the toxins. Under the same conditions, 10  $\mu\text{M}$  PH did not significantly modify the sucrose uptake capacity of the root tissues, however, it transiently inhibited the uptake in the leaf tissues. In this case, increasing the treatment duration from 3 to 6, 12, and 24 h inhibited sucrose uptake from 12, 29, 21 and 1%, respectively (**Fig. 7B**).

Comparative assays showed that valine uptake was also modified by the inhibitors with similar characteristics as in sucrose uptake, although with some differences in the extent of their action. The capacity of valine uptake by root and leaf tissues showed an aging process and was more affected in roots tissues treated with CB and CD than in leaf tissues (**Fig. 7C, D**). Increasing the treatment duration from 3 to 6, 12, and 24 h increased the inhibition of net valine uptake in the roots respectively from 29 to 36, 50 and 71% for 10  $\mu\text{M}$  CB and from 14 to 28, 25 and 35% for 10  $\mu\text{M}$  CD, respectively (**Fig. 7C**). Increasing the treatment duration from 3 to 6, 12, and 24 h increased uptake inhibition in the leaves from 19 to 20, 17, and 17% for 10  $\mu\text{M}$  CB and from 10 to 14, 10 and 7% for 10  $\mu\text{M}$  CD (**Fig. 7D**). Furthermore, CB and CD acted more rapidly on the valine uptake capacity, since a significant inhibition was observed after 3 h treatment duration. Note that 10  $\mu\text{M}$  PH did not significantly modify the uptake capacity of valine in roots and leaves. Notably, above the threshold value of 1  $\mu\text{M}$ , the inhibition of sucrose and valine uptake observed on root and leaf tissues treated for 12 h with CD and CB was dose-dependent (**Fig. 8A, B, C, D**).

### **Effect of cytochalasin B, cytochalasin D and phalloidin on the uptake of sucrose and valine by plasma membrane vesicles purified from root and leaf tissues**

The PMV model allows us to examine the sucrose transporter expressed in the mesophyll cells and in storage parenchyma cells of roots, which represent the more abundant cell type in the tissues. The use of the “energized” PMVs allowed to determine if the toxins may act on the activities of the transporters through a side effect, resulting from an inhibition of the cell metabolism. Proton motive force (pmf)-driven uptake of sucrose and valine was significantly reduced in PMVs from roots treated with CB (by 18% and 20%, respectively) and CD (by 18% and 31%, respectively), whereas it appeared to be significantly unaffected in PH-treated PMVs (**Fig. 9A, C**). Comparatively, the uptake of sucrose and valine was also significantly inhibited in PMVs purified from leaves treated with CB (18% and 15%, respectively), but was unaffected in PMVs treated with CD (**Fig. 9B, D**). However, PH inhibited sucrose uptake in PMVs purified from leaves, whereas it did not significantly affect valine uptake (**Fig. 9B, D**). Therefore, a close parallelism in the action of the compounds can be observed in tissues and in PMVs purified from

1  
2  
3 362 the respective tissues, strongly suggesting that the inhibitors acted directly through a modification  
4 363 at the plasma membrane level.  
5  
6 364

7  
8 365 **Effect of cytochalasin B, cytochalasin D and phalloidin on H<sup>+</sup>-ATPase activity**

9  
10 366 In order to verify that the different inhibitors did not act indirectly through a modification of the  
11 367 plasma membrane H<sup>+</sup>-ATPase activity, which energizes the H<sup>+</sup> co-transport of sugars and amino  
12 368 acids, we first assayed CB, CD and PH on the H<sup>+</sup> fluxes occurring in the plant tissues. As  
13 369 previously shown, a continuous acidification over a period of 5 h was observed in the incubation  
14 370 medium of root quarters, the pH decreasing from 6.3 to 5.5 (Michonneau et al. 2004). A similar  
15 371 observation has been made in the incubation medium of leaf tissues (Delrot 1981). In both  
16 372 experimental models, fusicoccin, a well-known H<sup>+</sup>-ATPase activator (Marrè 1979), increased the  
17 373 rate of acidification.

18  
19  
20 374 The results of the assays showed that the decrease in pH of the control medium containing the  
21 375 root and leaf tissues was similar to the observed trend in media containing CB, CD, and PH at the  
22 376 concentrations previously used in the uptake experiments, indicating that the excretion of protons  
23 377 was not altered in the treated tissues (results not shown). Additionally, we examined the effect of  
24 378 the direct application of the compounds on the PMVs on the H<sup>+</sup>-ATPase activity. CB, CD, and  
25 379 PH used at low concentrations (1 μM and 10 μM), did not significantly modify the transmembrane  
26 380 proton pumping and the vanadate-sensitive enzyme catalytic activity of the vesicles; however, the  
27 381 inhibition of both activities was induced at 50 μM (Table 1).

28  
29  
30 382 Taken together, our results indicated that CB, CD, and PH did not affect the uptake of sucrose  
31 383 and valine at the concentration used through a side effect by acting on the H<sup>+</sup>-ATPase, but  
32 384 achieved their inhibitory effect by acting directly on a physiological process that regulates the  
33 385 activity of the transporters.  
34  
35  
36  
37  
38  
39  
40  
41  
42  
43  
44  
45  
46  
47  
48  
49  
50  
51  
52  
53  
54  
55  
56  
57  
58  
59  
60

## Discussion

### Differential effects of cytochalasins and phalloidin on sucrose and valine uptake

Previous studies have shown that the uptake of sucrose and amino acids occurs through an active process mediated by plasma membrane carriers which used an H<sup>+</sup>-substrate co-transport mechanism in leaf cells (Delrot et al. 1980, Bush 1989, Lemoine and Delrot 1989) and tap root cells (Michonneau et al. 2004). The presence of carriers supports the idea that nutrient fluxes are apoplastic (without ruling out the symplastic way). The mesophyll cells in plants behave like sources and are involved in unloading processes before the loading of sucrose and amino acids in the phloem cells for long-distance transport. However, under the experimental conditions used in the present study, the leaf disc model has been widely used to study the mechanisms of nutrient transport with significant results (Delrot 1981, Sakr et al. 1993). Under these conditions, the direction of transport may be reversed depending on the direction of the nutrient gradient, pH or transmembrane potential, as reported for ZmSUT1, the sucrose carrier in *Zea mays* (Carpaneto et al. 2005).

Our results showed that the pattern of sucrose and valine uptake was organ-specific. The capacity of valine uptake was however 3- and 2-fold higher than that of sucrose uptake, as well in the roots as in the leaves as previously noted (Sakr et al. 1997, Michonneau et al. 2004). Nevertheless, the uptake pattern had some similarities, particularly, the uptake capacity asymptotes at 12 h, indicating that a net loss of substrate pool sizes occurred through either metabolic use or leakage back to the medium.

CB, CD, and PH differentially modified nutrient transport in beet plant tissues. CB had a stronger inhibitory on sucrose and valine uptake in both roots and leaves than CD. In contrast, PH had no effect, except on sucrose uptake in leaf tissues. Furthermore, the uptake of sucrose and valine was more inhibited in the root cells by CB and CD than in the leaf cells, suggesting that nutrient transport regulation differs in mesophyll and root storage cells. Similarities in the modification of sugar transport by the toxins used can be drawn from comparative data reported on animal cells. The different toxins examined have been extensively used as tools to determine the characteristics of sugar transport in several animal cell models. In particular, CB has been shown to inhibit the transport of glucose in several mammalian cell lines (Mizel and Wilson 1972), to reversibly alter hexose transport, glucosamine (Allen et al. 1980), a D-2-deoxyglucose uptake in leucocytes and fibroblasts (Zigmond and Hirsch 1972) and sugars in erythrocytes (Lin and al. 1978), in enterocytes (Uezato and Fujita 1986), and renal cells (Silverman and Turner 1982, Cheung and Hammerman 1988). Additionally, studies have reported that the action of CD is reduced in red blood cells (RBC) sugar transport compared with the action of CB (Leitch and

1  
2  
3 423 Carruthers, 2009) and this observation has been linked with the lower binding affinity of CD to  
4 424 the GLUT1 transporter (Rampal et al. 1980, Leitch and Carruthers 2009).

5 425

6 426  
7  
8 427 **Possible effect of the toxins on sucrose uptake through a direct action on the**  
9 **transporter**

10 428 Since the plasma membrane H<sup>+</sup>-ATPase activity in PMVs was not modified by the toxins at the  
11 429 concentrations used (Table 1), the observed inhibitory action on sucrose uptake cannot be  
12 430 ascribed to an indirect effect, such as the modification of the driving pmf. Therefore, in light of  
13 431 the knowledge concerning the effects of the toxins on animal cells, it can be assumed that the  
14 432 toxins had a direct effect on the transporters. However, there is need for further studies on plant  
15 433 materials. Several studies have shown that the activity of GLUT family of transporters, which  
16 434 were localized in various tissues, was inhibited by CB at the concentration used in this work  
17 435 (Kellett et al. 2008, Augustin 2010). Previous studies have reported that in glucose transport in  
18 436 erythrocytes which is mediated by the transport protein GLUT1 (Mueckler et al. 1985), CB acted  
19 437 as an endofacial site inhibitor in the RBCs (Krupka and Devés, 1980) and renal proximal tubular  
20 438 cells (Cheung and Hammerman 1989). Jung and Rampal (1977) showed that CB binding to PMVs  
21 439 from RBC is multisite and a site, corresponding to the functional GLUT1 transport, accounts for  
22 440 30% of the total CB binding sites. In the second mode of glucose uptake which has been observed  
23 441 particularly in intestine and kidney cells, glucose absorption was achieved through sodium-  
24 442 dependent sugar transporters (SGLTs), and the glucose is co-transported with Na<sup>+</sup> via an  
25 443 electrochemical gradient across the membrane, which is maintained by the Na<sup>+</sup>/K<sup>+</sup> pump (Kellett  
26 444 et al. 2008, Harada and Inagaki 2012). Characteristically, this co-transport is directly inhibited by  
27 445 the plant glucoside phloridzin which is reported to be a potent competitive inhibitor of glucose  
28 446 transport in intestine and kidney cells (Wright et al. 2011). Although phloridzin has been shown  
29 447 to inhibit the uptake of glucose and sucrose in broad bean tissue (Lemoine et al. 1987), the  
30 448 inhibition of sucrose and valine uptake observed in the present study could not be attributed to  
31 449 SGLTs without undertaking further analysis. This is because we have observed that phloridzin  
32 450 had a high inhibitory effect on proton pumping and the H<sup>+</sup>-ATPase activity of PMVs from beet  
33 451 leaves at a concentration of 5 mM (unpublished data). Therefore, the observed inhibition of uptake  
34 452 following phloridzin application may be due to the strong protonophore effect of the compound.

35 453 Western blot analysis conducted with the AtSUC1 antibody revealed one band at 42 kDa in  
36 454 the leaf cells, confirming the results of Gallet et al. (1992), Sakr et al. (1997) and Li et al. (1994).  
37 455 A supplementary isoform was observed at 56 kDa in the tap root cells. Similarly, a band  
38 456 corresponding to a sucrose carrier was observed at 55 kDa in the leaves of *Spinacea oleracea*  
39 457 (SoSUT1) (Riesmeier et al. 1992), at 54 kDa in the leaves of *Plantago major* (PmSUT2) (Gahrtz  
40 458 et al. 1994) and *Solanum tuberosum* (Krügel et al. 2008), and at 50 kDa in the leaves of *B. vulgaris*  
41 459 (Nieberl et al. 2017). Therefore, we cannot exclude the fact that the antibody recognized the two

1  
2  
3 460 different sucrose transporters expressed in the different cell types. Therefore, it can be inferred  
4 461 that the higher inhibitory effect of CB on sucrose uptake in roots may be linked to the CB binding  
5 462 to the 56 kDa component.  
6 463

### 10 464 **Possible effect of the toxins on nutrient uptake by modifying the functionality of the** 11 465 **cytoskeleton**

12  
13 466 The effect of CB and CD cannot be restricted to inhibition of the activity of the sucrose  
14 467 transporter, as evidenced by their strong inhibitory effect also observed on amino acid uptake.  
15 468 This led us to believe that a component of the compounds' action may be linked to a general  
16 469 plasma membrane process. The inhibition of the uptake of valine and sucrose by CB and CD  
17 470 showed a similar trend; however, their inhibitory effect was stronger in root cells than in leaf  
18 471 cells. Contrarily, PH did not significantly inhibit the uptake of sucrose and valine in the  
19 472 experimental samples. Furthermore, the lack of specificity in the action of CB on sugar transport  
20 473 has been previously reported in some animal cells (Estensen et al., 1972). Zhang and Ismail-Beigi  
21 474 (1988) suggested that the toxins (CB, CD, and PH) do not only act specifically on the transporters  
22 475 GLUT1, GLUT2, but bind to membranes and modify the organization of the cytoskeleton. They  
23 476 reported that the binding of cytochalasin E (CE) to actin filament resulted in a conformational  
24 477 change in proteins that are closely associated with GLUT1, leading to the unmasking of the  
25 478 transporter. Additionally, it has been shown in RBCs that 30 % of the total CB binding sites  
26 479 correspond to actin sites (Jung and Rampal 1977). Similarly, cytoskeletal rearrangement has been  
27 480 linked with the activity of Na<sup>+</sup>-dependent sugar transporter SGLT1 in kidney and intestinal cells  
28 481 (Hediger et al. 1987, Pappenheimer et al. 1987, Kellett et al. 2008). Furthermore, Diez and  
29 482 Sanpedro (2000) reported that the inhibitory effect of CE on the intestinal SGLT1 was secondary  
30 483 to its action on the cytoskeleton through protein structure modification.

31 484 Generally, in light of the effects induced by the different tested toxins on the processes of  
32 485 cytokinesis and cell motility, these reports lead to the consideration of the general role played by  
33 486 microfilaments in plant cell physiology (Pollard and Borisy 2003). Actin filaments are widespread  
34 487 (Parthasarathy et al. 1985) and form a network, which is closely bound to the plasma membrane  
35 488 and influence the functioning of intrinsic membrane proteins through topographic modifications  
36 489 and the specific dynamics of the plasma membrane (Lopez et al., 1994). Besides its involvement  
37 490 in cytoplasmic streaming which allows movements of vesicles and organelles (Williamson 1979,  
38 491 Parthasarathy et al. 1985, Staiger and Schliva 1987), actin is known to intervene in the structural  
39 492 integrity of the plasma membrane/cytosol interface in plant cells (Schmit and Lambert 1988). The  
40 493 accumulation of sucrose in the vacuole of root storage cells induces the development of a strong  
41 494 osmotic pressure (900 mosmol) (Leigh et al. 1979), which may result in a compressive stress on  
42 495 the thin cytoplasm layer (less than 1  $\mu\text{m}$  thick) orthogonally to the wall. This situation in root  
43  
44  
45  
46  
47  
48  
49  
50  
51  
52  
53  
54  
55  
56  
57  
58  
59  
60

1  
2  
3 496 cells should be associated with an original cytoskeleton organization, which may control the  
4  
5 497 balance between vacuole and wall pressures. Therefore, a modification of the cytoskeleton  
6  
7 498 structure may affect the membrane processes involved in exchanges between the symplast and  
8  
9 499 apoplast. The short distance (averaged 40 nm; **Fig. 6**) between actin and AtSUC1 sites, which  
10  
11 500 were identified by the gold-labeled antibodies, suggests that a functional relationship may exist  
12  
13 501 between the sucrose carrier and actin microfilaments in the vicinity of the plasma membrane. This  
14  
15 502 short distance may be occupied by actin binding proteins that regulate the assembly/disassembly  
16  
17 503 of actin monomers along the actin filaments (approximately 0.9 nm wide) and are also expected  
18  
19 504 to control the anchoring with cytoskeletal proteins such as villin, formin, myosin, and spectrin  
20  
21 505 (**Higaki et al. 2007, Martinière et al. 2011**), and possibly with plasma membrane transport  
22  
23 506 proteins. Additionally, **Tsakiridis et al. (1994)** reported that spectrin specifically associated with  
24  
25 507 GLUT4 transporter created a direct interaction between glucose transporter containing vesicles  
26  
27 508 and actin network. CD, which disassembled the actin network affected the recruitment of  
28  
29 509 preformed vesicles in intracellular organelles to the plasma membrane. Such a long-term effect  
30  
31 510 may be compatible with the observed time course of sucrose uptake inhibition in the present study  
32  
33 511 (**Fig. 7**).

34  
35 512 **Western blot analysis showed that actin was quantitatively more represented in root cells than**  
36  
37 513 **in leaf cells (Fig. 2).** This would explain in part why the drug action on actin microfilaments  
38  
39 514 affected the uptake capacity in the root cells more strongly than in the leaf cells. However, this  
40  
41 515 hypothesis should be further verified since only one isoform of actin was identified through the  
42  
43 516 western blot analysis, whereas plant actins are encoded by multigene families, leading to distinct  
44  
45 517 classes of tissue-specific actin RNA (**McLean et al. 1990**) which may encode actins with different  
46  
47 518 functions in roots and leaf cells. **Additionally, immunodetection of spectrin in PMVs from the**  
48  
49 519 **leaf and root tissues and the number of immunolocalized sites in TEM observations suggest that**  
50  
51 520 **the cytoskeleton of the roots is more extended than the cytoskeleton of the leaves**  
52  
53 521 **(Supplementary data 1).**

54  
55 522  
56  
57 523 Conclusively, the inhibitory effect of CB, CD, and PH on sucrose and valine uptake in mesophyll  
58  
59 524 and root cells of sugar beet may be exerted through two but not exclusive mechanisms related to  
60  
525 the nutrient transport in plant cells (binding to transporters and modification of the cytoskeleton  
526 organization). Whatever the mechanism involved, the observed moderate inhibition (not higher  
527 than 30% for sucrose uptake and 50% for valine) suggests that they do not act as main effectors  
528 of nutrient uptake but as modulators in transport processes. A working hypothesis could be that  
529 the carrier isoforms evidenced here are not linked in the same way with the actin network in roots  
530 and leaves. Thus, a future study should consider the possible involvement of actin-associated  
531 proteins in both plant tissues.  
532

1  
2  
3 533  
4

5 534

## Contributions

7  
8 535

PM involved in acquisition of physiological data

9 536

PFL Planned the study and involved in acquisition of microscopic data

10 537

AC involved in confocal observations and analyses

11 538

AC involved in bibliographical analysis and critical revision of the manuscript

12 539

JMB contributes to obtain fundings and to critical revision of the manuscript

13 540

GR involved in analysis and interpretation of the data

14 541

15 542

All authors wrote the manuscript and approved the final version

16 543

17 544

## Acknowledgments

18 545

The authors are grateful to Dr. Lemoine for his advices and improvement of the manuscript and acknowledge the "Service de Microscopie et d'Imagerie Scientifique (Image UP) of the University of Poitiers, in particular Emile Béré for his help in TEM observations. This work was partly granted by the following 2015–2020 programs: the State-Region Planning Contracts (CPER) and the European Regional Development Fund (FEDER).

19 550

20 551  
21  
22  
23  
24  
25  
26  
27  
28  
29  
30  
31  
32  
33  
34  
35  
36  
37  
38  
39  
40  
41  
42  
43  
44  
45  
46  
47  
48  
49  
50  
51  
52  
53  
54  
55  
56  
57  
58  
59  
60

552 **References**

- 553 Abu-Abied M, Golomb L, Belausov E, Huang S, Geiger B, Kam Z, Staiger CJ, Sadot E (2006)  
554 Identification of plant-cytoskeleton-interacting proteins by screening for actin stress fiber  
555 association in mammalian fibroblasts. *Plant J* 48: 367-379
- 556 Allen ED, Aiuto R, Sussman AS (1980) Effects of cytochalasins on *Neurospora crassa* - I. Growth  
557 and Ultrastructure. *Protoplasma* 102: 63-75
- 558 Augustin R (2010) The protein family of glucose transport facilitators: it's not only about glucose  
559 after all. *IUMB life* 62: 315-333
- 560 Bearden JC (1978) Quantification of submicrogram quantities protein by an improved-dye  
561 binding assay. *Biochim Biophys Acta* 533: 525-529
- 562 Bouché-Pillon S, Fleurat-Lessard P, Serrano R, Bonnemain JL (1994) Asymmetric distribution  
563 of the plasma-membrane H<sup>+</sup>-ATPase in embryos of *Vicia faba* L. with special reference to  
564 transfer cells. *Planta* 193: 392-397
- 565 Bush DR (1989) Proton-coupled sucrose transport in plasmalemma vesicles isolated from sugar  
566 beet (*Beta vulgaris* L. cv Great Western) leaves. *Plant Physiol* 89: 1318-1323
- 567 Bush DR (1990) Electrogenicity, pH-dependence, and stoichiometry of the proton-sucrose  
568 symport. *Plant Physiol* 93: 1590-1593
- 569 Carpaneto A, Geiger D, Bamberg E, Sauer N, Fromm J, Hedrich R (2005) Phloem-localized,  
570 proton-coupled sucrose carrier ZmSUT1 mediates sucrose efflux under the control of the  
571 sucrose gradient and the proton motive force. *J Biol Chem* 280: 21437-21443
- 572 Casella JF, Flanagan MD, Lin S (1980) Cytochalasin D inhibits actin polymerization and induces  
573 depolymerization of actin filaments formed during platelet shape change. *Nature* 293: 302-  
574 305
- 575 Chen L-Q (2014) Sweet sugar transporters for phloem transport and pathogen nutrition. *New*  
576 *Phytol.* 201: 1150-1155.
- 577 Cheung PT, Hammerman MR (1989) Cytochalasin B binding to rabbit proximal tubular  
578 basolateral membranes. *Kidney Internat* 35: 1290-1294
- 579 Cooper JA (1987) Effects of cytochalasin and phalloidin on actin. *J Cell Biol* 105: 1473-1478

- 1  
2  
3 580 Deeks MJ, Calcutt, JR, Ingle EKS, Hawkings TJ, Chapman S, Richardson AC, Mentlak DA,  
4 581 Dixon MR, Cartwright F, Smertenko AP, Oparka K, Hussey PJ (2012) A superfamily of actin-  
5 582 binding proteins at the actin-membrane Nexus of higher plants. *Curr Biol* 22: 1595-1600  
6  
7  
8 583 Delrot S (1981) Proton fluxes associated with sugar uptake in *Vicia faba* leaf tissues. *Plant*  
9 584 *Physiol* 68: 706-711  
10  
11  
12 585 Delrot S, Despeghel JP, Bonnemain JL (1980) Phloem loading in *Vicia faba* leaves: effect of n-  
13 586 ethylmaleimide and parachloromercuribenzenesulfonic acid on H<sup>+</sup> extrusion, K<sup>+</sup> and sucrose  
14 587 uptake. *Planta* 149: 144-148  
15  
16  
17 588 Diez-Sampedro A., Lostao MP, Barber A (2000) Cytoskeleton involvement on intestinal  
18 589 absorption processes. *J Physiol Biochem* 56: 25-32  
19  
20  
21 590 Esau K., Thorsch J (1985) Sieve plate pores and plasmodesmata, the communication channels of  
22 591 the symplast: ultrastructural aspect and developmental relations. *Amer J Bot* 1: 1641-1653  
23  
24  
25 592 Estensen RD, Plagemann PG (1972) Cytochalasin B: inhibition of glucose and glucosamine  
26 593 transport. *Proc Natl Acad Sci USA* 69: 1430-1434  
27  
28  
29 594 Feuerstein A, Niedermeier M, Bauer K, Engelmann S, Hoth S, Stadler R, Sauer N (2010)  
30 595 Expression of the *AtSUC1* gene in the female gametophyte, and ecotype-specific expression  
31 596 differences in male reproductive organs. *Plant Biol* 12 (Suppl 1): 105-114  
32  
33  
34 597 Fleurat-Lessard P, Vantard M, Schmit AC, Stoeckel H, Roblin G (1993) Characterization and  
35 598 immunocytochemical distribution of microtubules and F-actin filament in protoplasts of  
36 599 *Mimosa pudica* motor cells. *Plant Physiol Biochem* 31: 757-764  
37  
38  
39 600 Fleurat-Lessard P, Frangne N, Maeshima M, Ratajczak R, Bonnemain JL, Martinoia E (1997)  
40 601 Increased expression of vacuolar aquaporin and H<sup>+</sup>-ATPase related to motor cell function in  
41 602 *Mimosa pudica* L. *Plant Physiol* 114: 827-834  
42  
43  
44 603 Gahrtz M, Stolz L, Sauer N (1994) A phloem-specific sucrose-H<sup>+</sup> symporter from *Plantago*  
45 604 *major* L. supports the model of apoplastic phloem loading. *Plant J* 6: 17-23  
46  
47  
48 605 Gallagher SR, Leonard RT (1982) Effect of vanadate, molybdate and azide on membrane-  
49 606 associated ATPase and soluble phosphatase activities of corn roots. *Plant Physiol* 70: 1335-  
50 607 1440  
51  
52  
53 608 Gallet O, Lemoine R, Delrot, S (1989) The sucrose carrier of the plant plasma membrane. I.  
54 609 Differential affinity labeling. *Biochim Biophys Acta* 978: 56-64  
55  
56  
57  
58  
59  
60

- 1  
2  
3 610 Gallet O, Lemoine R, Gaillard C, Larsson C, Delrot S (1992) Selective inhibition of active uptake  
4 611 of sucrose into plasma membrane vesicles by polyclonal sera directed against a 42 kilodalton  
5 612 plasma membrane polypeptide. *Plant Physiol* 98: 17-23  
6  
7  
8 613 Giaquinta RT (1977) Possible role of pH gradient and membrane ATPase in the loading of  
9 614 sucrose into the sieve tubes. *Nature* 267: 369-370  
10  
11  
12 615 Harada N, Inagaki N (2012) Role of sodium-glucose transporter in glucose uptake of the intestine  
13 616 and kidney. *J Diabetes Invest* 3: 352-353  
14  
15  
16 617 Hardham AR, Jones DA, Takemoto D (2007) Cytoskeleton and cell wall function in penetration  
17 618 resistance. *Curr Opin Plant Biol* 10: 342-348  
18  
19  
20 619 Hediger MA, Coady MJ, Ikeda TS, Wright EM (1987) Expression cloning and cDNA sequencing  
21 620 of the Na<sup>+</sup>/glucose transporter. *Nature* 330: 379-381  
22  
23  
24 621 Higaki T, Sano T, Hasezawa S (2007a) Actin microfilament dynamics and actin side-binding  
25 622 proteins in plants. *Curr Opin Plant Biol* 10: 549-556  
26  
27  
28 623 Higaki T, Goh T, Hayashi T, Kutsuna N, Kadota Y, Hasezawa S, Sano T, Kuchitsu K (2007b)  
29 624 Elicitor-induced cytoskeletal rearrangement relates to vacuolar dynamics and execution of cell  
30 625 death: *in vivo* imaging of hypersensitive cells death in tobacco BY-2 cells. *Plant Cell Physiol*  
31 626 48: 1414-1425  
32  
33  
34 627 Hussey PJ, Ketelaar T, Deeks MJ (2006) Control of the actin cytoskeleton in plant cell growth.  
35 628 *Annu Rev Plant Biol* 57: 109-125  
36  
37  
38 629 Jung CY, Rampal AL (1977) Cytochalasin B binding sites and glucose transport carrier in human  
39 630 erythrocyte ghosts. *J Biol Chem* 252: 456-5463  
40  
41  
42 631 Jung B, Ludewig F, Schulz A, Meißner G, Wöstefeld N, Flüge U-I, Pommerrenig B, Wirsching  
43 632 P, Sauer N, Koch W, Sommer F, Mühlhaus T, Schroda M, Cui TA, Graus D, Marten I,  
44 633 Hedrich R, Neuhaus KE (2015) Identification of the transporter responsible for sucrose  
45 634 accumulation in sugar beet taproots. *Nature Plants* 1: 14001  
46  
47  
48  
49 635 Kandasamy M, Meagher RB (1999) Actin-organelle interaction: association with chloroplast in  
50 636 *Arabidopsis* leaf mesophyll cells. *Cell Motil Cytoskeleton* 44, 110-118  
51  
52  
53 637 Kellett GL, Brot-Laroche E, Mace OJ, Leturque A (2008) Sugar absorption in the intestine: the  
54 638 role of GLUT2. *Annu Rev Nutrition* 28: 35-54  
55  
56  
57 639 Kijima ST, Hirose K, Kong S-G, Wada M, Uyeda TQP (2016) Distinct biochemical properties of  
58 640 *Arabidopsis thaliana* actin isoforms. *Plant Cell Physiol* 57: 46-56  
59  
60

- 1  
2  
3 641 Krügel U, Veenhoff LM, Langbein J, Wiederhold E, Liesche J, Friedrich T, Grimm B, Martinoia  
4 642 E, Poolman B, Kühn (2008) Transport and sorting of the *Solanum tuberosum* sucrose  
5 643 transporter SUT1 is affected by posttranslational modification. *Plant Cell* 20: 2497-2513  
6  
7  
8 644 Krupka RM, Devés R (1980) Testing transport systems for competition between pairs of  
9 645 reversible inhibitors. *J Biol Chem* 255 : 11870-11874  
10  
11  
12 646 Lachaud S (1964) La croissance en épaisseur de l'hypocotyle de *Beta vulgaris* L. et les  
13 647 modifications que peut y provoquer l'acide gibbérellique. *C R Séanc Soc Biol* 158: 348-350  
14  
15  
16 648 Laemmli UK (1970) Cleavage of structural proteins during the assembly of the head of  
17 649 bacteriophage T4. *Nature* 227: 680-685  
18  
19  
20 650 Laurel AM, Lucas WJ (1996) Plasmodesmal cell-to-cell transport of proteins and nucleic acids.  
21 651 *Plant Molec Biol* 32: 251-273  
22  
23  
24 652 Leigh RA, Rees T, Fuller WA, Banfield J (1979) The location of acid invertase activity and  
25 653 sucrose in the vacuole of storage roots of beetroot (*Beta vulgaris*). *Biochem J* 178: 539-547.  
26  
27  
28 654 Leitch JM, Carruthers A (2009)  $\alpha$ - and  $\beta$ -monosaccharide transport in human erythrocytes. *Amer*  
29 655 *J. Physiol. Cell Physiol* 296: C151-C161  
30  
31  
32 656 Lemoine R (2000) Sucrose transporters in plants: update on function and structure. *Biochim*  
33 657 *Biophys Acta* 1465: 246-262  
34  
35  
36 658 Lemoine R, Delrot S (1987) Recognition of phlorizin by the carriers of sucrose and hexose in  
37 659 broad bean leaves. *Physiol Plant* 69: 639-644  
38  
39  
40 660 Lemoine R, Delrot S (1989) Proton motive force-driven sucrose uptake in sugar beet plasma  
41 661 membrane vesicles. *FEBS Lett* 249: 129-133  
42  
43  
44 662 Lemoine R, Bourquin S, Delrot S (1991) Active uptake of sucrose by plant PMV: determination  
45 663 of some important physical and energetical parameters. *Physiol Plant* 82: 377-384  
46  
47  
48 664 Lemoine R, Kühn C, Thiele N, Delrot S, Frommer WB (1996) Antisense inhibition of the sucrose  
49 665 transporter: effect on amount of carrier and sucrose transport activity. *Plant Cell Environ* 19:  
50 666 1124-1131  
51  
52  
53 667 Li ZS, Noubahni AM, Bourbouloux A, Delrot S (1994) Affinity purification of sucrose binding  
54 668 protein from the plant plasma membrane. *Biochim Biophys Acta* 1219: 389-397  
55  
56  
57 669 Lin S, Lin DC, Flanagan MD (1978) Specificity of the effects of cytochalasin B on transport and  
58 670 motile processes. *Proc Natl Acad Sci USA* 75: 329-333  
59  
60

- 1  
2  
3 671 Lopez A, de Bony J, Dupou-Cezanne L, Tournier JF, Schram V, Welby M, Tocanne JF (1994)  
4 672 Organisation latérale, dynamique translationnelle et percolation dans les membranes  
5 673 biologiques. De la matière du vivant. Les systèmes moléculaires organisés. CNRS-Images de  
6 674 la Recherche 2: 103-106
- 7  
8  
9  
10 675 Lucas WJ, Ding B, Van Der Schoot C (1993) Plasmodesmata and the supracellular nature of  
11 676 plants. *New Phytol* 125: 435-476
- 12  
13  
14 677 Marrè E (1979) Fusicoccin: a tool in plant physiology. *Annu Rev Plant Physiol* 30: 273-288
- 15  
16 678 Martinière A, Gayral P, Hawes C, Runions J (2011) Building bridges: formin1 of Arabidopsis  
17 679 forms a connection between the cell wall and the actin cytoskeleton. *Plant J* 66: 354-365
- 18  
19  
20 680 McLean BG, Eubanks S, Meagher R (1990) Tissue specific expression of divergent actins in  
21 681 soybean root. *Plant Cell* 2: 335-344
- 22  
23  
24 682 Michaud D, Guillet G, Rogers PA, Charest PM (1991) Identification of a 220 kDa membrane-  
25 683 associated plant cell protein immunologically related to human  $\beta$ -spectrin. *FEBS Lett* 294: 77-  
26 684 80
- 27  
28  
29 685 Michonneau P, Roblin G, Bonmort J, Fleurat-Lessard P (2004) Valine uptake in the tap root of  
30 686 sugar beet: a comparative analysis with sucrose uptake. *J Plant Physiol.* 161: 1299-1314
- 31  
32  
33 687 Mizel SB, Wilson L (1972) Inhibition of the transport of several hexoses in mammalian cells by  
34 688 cytochalasin B. *J Biol Chem* 247: 4102-4105
- 35  
36  
37 689 Mueckler M, Caruso C, Baldwin SA, Panico M, Blench I, Morris HR, Allard WJ, Lienhard GE,  
38 690 Lodish HF (1985) Sequence and structure of a human glucose transporter. *Science* 229: 941-  
39 691 945
- 40  
41  
42 692 Nieberl P, Ehrl C, Pommerrenig B, Graus D, Marten I, Jung B, Ludewig F, Koch W, Harms K,  
43 693 Flügge U-I, Neuhaus HE, Hedrich R, Sauer N (2017) Functional characterization and cell  
44 694 specificity of BvSUT1, the transporter that loads sucrose into the phloem of sugar beet (*Beta*  
45 695 *vulgaris* L.) source leaves. *Plant Biol* 19, 315-326
- 46  
47  
48  
49 696 Noubahni AM, Sakr S, Denis MH, Delrot S (1996) Transcriptional and post-transcriptional  
50 697 control of the plasma membrane H<sup>+</sup>-ATPase by mechanical treatments. *Biochim Biophys Acta*  
51 698 1281: 213-219
- 52  
53  
54  
55 699 O'Neill SD, Spanswick RM (1984) Effects of vanadate on the plasma membrane ATPase of red  
56 700 beet and corn. *Plant Physiol* 75: 586-591
- 57  
58 701  
59  
60

- 1  
2  
3 702 Pappenheimer JR, Reiss KZ (1987) Contribution of solvent drag through intracellular junctions  
4 703 to absorption of nutrients by the small intestine of the rat. *J Membr Biol* 100: 123-126  
5  
6 704 Parthasarathy MV, Perdue TD, Witztum A, Alvernaz J (1985) Actin network as a normal  
7 705 component of the cytoskeleton in many vascular plant cells. *Amer J Bot* 72: 1318-1323  
8  
9  
10 706 Pollard TD, Borisy GG (2003) Cellular motility driven by assembly and disassembly of actin  
11 707 filaments. *Cell* 112: 453-465  
12  
13  
14 708 Rampal AL, Pinkovsky HB, Jung CY (1980) Structure of cytochalasins and cytochalasin B  
15 709 binding sites in human erythrocyte membranes. *Biochemistry* 19: 679-683  
16  
17  
18 710 Riesmeier JW, Willmitzer L, Frommer WB (1992) Isolation and characterization of a sucrose  
19 711 carrier cDNA from spinach by functional expression in yeast. *EMBO J* 11: 4705-4713  
20  
21 712 Sakr S, Lemoine R, Gaillard C, Delrot S (1993) Effect of cutting on solute uptake by plasma  
22 713 membrane vesicles from sugar beet (*Beta vulgaris* L.) leaves. *Plant Physiol* 103: 49-58  
23  
24  
25 714 Sakr S, Noubahni M, Bourbouloux A, Riesmeier J, Frommer WB, Sauer N, Delrot S (1997)  
26 715 Cutting, ageing and expression of plant membrane transporters. *Biochim Biophys Acta* 1330:  
27 716 207-216  
28  
29  
30 717 Sauer N (2007) Molecular physiology of higher plant sucrose transporters. *FEBS Lett* 581: 2309-  
31 718 2317  
32  
33  
34 719 Sauer N, Stolz J (1994) SUC1 and SUC2: two sucrose transporters from *Arabidopsis thaliana*;  
35 720 expression and characterization in baker's yeast and identification of the histidine-tagged  
36 721 protein. *Plant J* 6: 67-77  
37  
38  
39 722 Schmit AC, Lambert AM (1988) Plant actin filament and microtubule interactions during  
40 723 anaphase-telophase transition: effects of antagonist drugs. *Biol Cell* 64: 309-319  
41  
42  
43 724 Serrano R (1989) Structure and function of plasma membrane ATPase. *Annu Rev Plant Physiol*  
44 725 *Plant Molec Biol* 40: 61-84  
45  
46  
47 726 Silverman M, Turner RJ (1982) 2-deoxy-D-glucose transport in dog kidney. *Amer J Physiol* 242:  
48 727 F711-720  
49  
50  
51 728 Sivitz AB, Reinders A, Ward JM (2008) Arabidopsis sucrose transporter AtSUC1 is important  
52 729 for pollen germination and sucrose-induced anthocyanin accumulation. *Plant Physiol* 147: 92-  
53 730 100  
54  
55  
56 731 Snyder FW, Carlson GE (1978) Photosynthate partitioning in sugar beet. *Crop Sci* 18: 657-669  
57  
58  
59  
60

- 1  
2  
3 732 Staiger CJ, Schliwa M (1987) Actin localisation and function in higher plants. *Protoplasma* 141:  
4 733 1-12  
5  
6  
7 734 Sze H (1985) H<sup>+</sup>-translocating ATPases: advances using membrane vesicles. *Annu Rev Plant*  
8 735 *Physiol* 36: 175-198  
9  
10  
11 736 Tian M, Chaudry F, Ruzicka DR, Meagher RB, Staiger CJ, Ray B (2009) Arabidopsis actin-  
12 737 depolymerizing factor AtADF4 mediates defense signal transduction triggered by the  
13 738 *Pseudomonas syringae* effector AvrPphB. *Plant Physiol* 150: 815-824  
14  
15  
16 739 Towbin H, Staehelin T, Gordon J (1979) Electrophoretic transfer of protein from polyacrylamide  
17 740 gels to nitrocellulose sheets: procedure and some applications. *Proc Natl Acad Sci USA* 76:  
18 741 4350-4354  
19  
20  
21 742 Tsakiridis T, Vranic M, Klip A (1994) Disassembly of the actin network inhibits insulin-  
22 743 dependent stimulation of glucose transport and prevents recruitment of glucose transporters to  
23 744 the plasma membrane. *J Biol Chem* 269: 29934-29942  
24  
25  
26  
27 745 Uezato T, Fujita M (1986) Cytochalasin B-binding proteins related to glucose transport across the  
28 746 basolateral membrane of the intestinal epithelial cell. *J Cell Sci* 85: 177-185  
29  
30  
31 747 Van Bel AJE, Gamalei Y (1991) Multiprogrammed phloem loading. In: Bonnemain, JL, Delrot  
32 748 S, Lucas WJ, Dainty J (eds), *Recent advances in phloem transport and assimilate*  
33 749 *compartmentation*, Ouest Editions, Presses Académiques, Nantes, pp. 128-139  
34  
35  
36 750 Van Bel AJE, Kempers R (1990) Symplastic isolation of the sieve element-companion cell  
37 751 complex in the phloem of *Ricinus communis* and *Salix alba* stems. *Planta* 183: 69-76  
38  
39  
40 752 Van Gestel K, Köhler RH, Verbelen J-P (2002) Plant mitochondria move on F-actin, but their  
41 753 positioning in the cortical cytoplasm depends on both F-actin and microtubules. *J Exp Bot* 53:  
42 754 659-667  
43  
44  
45 755 Vaughn MW, Harrington GN, Bush DR (2002) Sucrose-mediated transcriptional regulation of  
46 756 sucrose symporter activity in the phloem. *Proc Natl Acad Sci USA* 99: 10876-10880  
47  
48  
49 757 Williamson RE (1979) Actin in motile and other processes in plants cells. *Can J Bot* 58: 766-772  
50  
51 758 Wright EM, Loo DDF, Hirayama BA (2011) Biology of human sodium glucose transporters.  
52 759 *Physiol Rev* 91: 733-794  
53  
54  
55 760 Wyse RE, Zamski E, Deri Tomos A (1986) Turgor regulation of sucrose transport in sugar beet  
56 761 taproot tissues. *Plant Physiol* 81: 478-481  
57  
58  
59  
60

- 1  
2  
3 762 Zhang JZ, Ismail-Beigi F (1998) Activation of Glu1 transporter in human erythrocytes. Arch  
4 Biochem Biophys 356: 86-92  
5 763  
6  
7 764 Zigmond SH, Hirsh JG (1972) Cytochalasin B inhibition of D-2-deoxyglucose transport into  
8 leukocytes and fibroblasts. Science 176: 1432-1434  
9 765  
10  
11 766  
12  
13 767  
14  
15  
16  
17  
18  
19  
20  
21  
22  
23  
24  
25  
26  
27  
28  
29  
30  
31  
32  
33  
34  
35  
36  
37  
38  
39  
40  
41  
42  
43  
44  
45  
46  
47  
48  
49  
50  
51  
52  
53  
54  
55  
56  
57  
58  
59  
60

For Peer Review

1  
2  
3 769 **Legends of the figures**  
4

5 770 **Figure 1.** (A) The *Beta vulgaris* plants used in the present study at early developmental stage  
6 (120 days) showing a 2 cm-wide root and seven exporting leaves. (B) Autoradiography of a root  
7 771 disc quarter showing the distribution of radioactive  $^{14}\text{C}$ [sucrose], in the vascular bundles (VB,  
8 772 strong white labeling) and in the storage cell area (SC, faint white labeling) after 1 hour  
9 773 absorption. (C) Cross-section of the vascular bundle area of the root concentric rings showing the  
10 774 xylem vessels (XV) surrounded by xylem parenchyma (XP), cambium with aligned cells (C),  
11 775 phloem tissue (PH) and the adjacent storage area with wide SCs. (D, D') Detail in transmission  
12 776 electron microscopy (TEM) of SCs showing a large vacuole (V) pressing the thin cytoplasm  
13 777 (arrow) and nucleus (N) against the wall (W). (E) Autoradiography of a leaf disc showing the  
14 778 distribution of radioactive  $^{14}\text{C}$ [sucrose], in the mesophyll veins (arrow, strong white labeling) and  
15 779 in adjacent parenchyma (faint white labelling) after 1 hour absorption. (F) Cross-section of a  
16 780 small leaf vein: xylem and phloem tissues surrounded by the bundle sheath (BS) are surrounded  
17 781 by the large mesophyll cells (M), (G) TEM of the longitudinal section of a palisade mesophyll  
18 782 cell containing many plastids (P), a wide nucleus and large vacuoles.  
19 783 Paraformaldehyde/Glutaraldehyde /OsO<sub>4</sub>/LRWhite. (C, F) Semi thin sections, toluidine blue  
20 784 staining, Zeiss Axioplan; (D, G) Ultrathin sections, uranyl/lead, TEM, Jeol 1010. Bars: (A) 1 cm,  
21 785 (B, E) 1 mm, (C, D, F, G) 20  $\mu\text{m}$ , (D') 30  $\mu\text{m}$ .  
22 786

23 787 **Figure 2.** Western blot analysis of protein extracted from plasma membrane vesicles (10.5  $\mu\text{g}/\mu\text{l}$   
24 788 of proteins) isolated from the root and leaf of *Beta vulgaris*. Immunoblotting with 1/200 anti-actin  
25 789 antibody reveals a band corresponding to an actin isoform at 42 kDa strongly labeled in the root  
26 790 but weakly in the leaf. Immunoblotting with 1/2000 diluted anti-AtSUC1 antibody reveals a 42  
27 791 kDa isoform strongly labeled in the root but weakly in the leaf. Note that two other bands at 46  
28 792 kDa (low labeling) and at 56 kDa (strong labeling) were also observed in the root extract. Control,  
29 793 purified actin. Western blot by ECL kit (ref: RPN 2109).  
30 794

31 795 **Figure 3.** Immunogold labeling of F-actin (A, D) and AtSUC1 (B, E) on plasma membrane  
32 796 vesicles (diameter 0.4 - 0.8  $\mu\text{m}$ ) purified from roots (A, B, C) and leaves (D, E, F) of sugar beet.  
33 797 Controls (C, F) obtained by primary antibody omission.  
34 798 Paraformaldehyde/Glutaraldehyde/OsO<sub>4</sub>/LRWhite. Ultrathin sections in transmission electron  
35 799 microscopy. Labeling by gold particles (15 nm diameter) indicated by arrows. Bars = 0.5  $\mu\text{m}$ .  
36 800

37 801 **Figure 4.** Detail of immunogold labeling (arrows) of actin (1/20 diluted ICN anti-actin) (A, D)  
38 802 and AtSUC1 (1/40 diluted) (B, E) and control by antibody omission (C, F) in root storage cells  
39 803 (A, B, C) and mesophyll cells (D, E, F) of sugar beet. V, vacuole; W, wall.  
40 804 Paraformaldehyde/Glutaraldehyde/OsO<sub>4</sub> / LRWhite. Site recognition by 15 nm diameter gold  
41 805 particles in transmission electron microscopy. Bars = 0.5  $\mu\text{m}$ .  
42 806

1  
2  
3 804 **Figure 5.** (A) Protoplast of storage cells in the tap root. (B) Red labeling of F-actin with  
4 rhodamine phalloidin (C) Immunolabeling of AtSUC1 in the plasma membrane (green by  
5 805 fluorescein isothiocyanate (FITC) detection), using 1/40 diluted antibody. (D) Co-labelling of F-  
6 806 actin and AtSUC1. (E) Control: antibody and rhodamine omission. (F) Protoplast of mesophyll  
7 807 cells containing many plastids (blue-green colored). (G) Red labeling of F-actin with rhodamine  
8 808 phalloidin. (H) Immunolabeling of AtSUC1 in the plasma membrane (green by FITC detection)  
9 809 using 1/40 diluted antibody. (I) Co-labeling of F-actin and AtSUC1. (J) Control: antibody and  
10 810 rhodamine omission. Paraformaldehyde/Glutaraldehyde. Zeiss Axioplan (A, F), Olympus  
11 811 confocal microscopy (B-E, G-J). Bars = 20µm.

12  
13  
14  
15  
16  
17  
18 813 **Figure 6.** Immuno-colabeling of AtSUC1 (gold particles of 10 nm diameter) and actin (gold  
19 814 particles of 5 nm diameter) performed on ultrathin sections of plasma membrane vesicles (ve)  
20 815 obtained from *Beta vulgaris* roots (A) and leaves (B), and in ultrathin sections of root parenchyma  
21 816 (D) and mesophyll cells (E). Recognized sites of both proteins are distributed along plasma  
22 817 membrane area but absent along the tonoplast. Plasma membrane and tonoplast are respectively  
23 818 indicated by black- and white dotted lines in absence of uranyl/lead contrast. cyt, cytoplasm; V,  
24 819 vacuole; W, wall. C: control: absence of labeling in plasma membrane vesicles when antibodies  
25 820 are omitted. Paraformaldehyde/Glutaraldehyde/OsO<sub>4</sub>/LRWhite. Ultrathin sections in  
26 821 transmission electron microscopy. Bars = 50 nm.

27  
28  
29  
30  
31  
32  
33 822 **Figure 7.** Uptake of 1 mM sucrose (A, B) and 1 mM valine (C, D) by discs harvested from storage  
34 823 root tissues (A, C) and leaf tissues (B, D) of sugar beet. Uptake (30 min. duration) was measured  
35 824 after the various time duration at 10 µM final concentration of cytochalasin B (CB), cytochalasin  
36 825 D (CD) and phalloidin (PH). Mean ± SE; n = 45 from three independent experiments.

37  
38  
39  
40 826 **Figure 8.** Inhibition of the uptake of 1 mM sucrose (A, C) and 1 mM valine (B, D) in the root  
41 827 (white bars) and leaf (dark bars) tissues of sugar beet treated for 12 h with various concentrations  
42 828 of CB (A, B) and CD (C, D). Mean ± SE; n = 45 from three independent experiments. Uptake  
43 829 duration: 30 min;

44  
45  
46  
47 830 **Figure 9.** Effect of cytochalasin B (CB), cytochalasin D (CD) and phalloidin (PH) applied at 10  
48 831 µM final concentration on the uptake of 1 mM sucrose (A, B) and 1 mM valine (C, D) by PMVs  
49 832 purified from root (A, C) and leaf tissues (B, D). Uptake duration: 3 min. Co: control. Mean ± SD;  
50 833 n = 6 independent experiments. Values given at the top of the bars represent the induced inhibition  
51 834 (%).

52  
53  
54  
55 835

56  
57  
58 836  
59  
60

**Table 1:** Effects of cytochalasin B (CB), cytochalasin D (CD) and phalloidin (PH) on proton pumping and vanadate-sensitive ATPase activity of plasma membrane vesicle (PMVs) purified from roots and leaves of *Beta vulgaris*. n: number of measurements from three independent PMV preparations. Mean  $\pm$  SD. \*, significantly different from the control at P = 0.05 with the Student-Fisher *t* test.

<b>Proton pumping (OD units mg protein<sup>-1</sup> min<sup>-1</sup>) in PMVs purified from roots</b>				
	<b>n</b>	<b>CB</b>	<b>CD</b>	<b>PH</b>
Control	12	0.576 $\pm$ 0.088		
1 $\mu$ M	6	0.600 $\pm$ 0.087	0.568 $\pm$ 0.032	0.552 $\pm$ 0.088
10 $\mu$ M	6	0.552 $\pm$ 0.024	0.560 $\pm$ 0.072	0.554 $\pm$ 0.104
50 $\mu$ M	6	0.408 $\pm$ 0.024*	0.410 $\pm$ 0.080*	0.240 $\pm$ 0.016*
<b>Proton pumping (OD units mg protein<sup>-1</sup> min<sup>-1</sup>) in PMVs purified from leaves</b>				
	<b>n</b>	<b>CB</b>	<b>CD</b>	<b>PH</b>
Control	12	0.373 $\pm$ 0.020		
1 $\mu$ M	6	0.377 $\pm$ 0.024	0.342 $\pm$ 0.008	0.334 $\pm$ 0.061
10 $\mu$ M	6	0.360 $\pm$ 0.023	0.390 $\pm$ 0.060	0.412 $\pm$ 0.043
50 $\mu$ M	6	0.260 $\pm$ 0.024*	0.277 $\pm$ 0.080*	0.282 $\pm$ 0.022*
<b>ATPase activity (nmol Pi mg protein<sup>-1</sup> min<sup>-1</sup>) in PMVs purified from roots</b>				
	<b>n</b>	<b>CB</b>	<b>CD</b>	<b>PH</b>
Control	12	391 $\pm$ 56		
1 $\mu$ M	8	437 $\pm$ 55	467 $\pm$ 96	425 $\pm$ 62
10 $\mu$ M	6	430 $\pm$ 30	405 $\pm$ 30	401 $\pm$ 36
50 $\mu$ M	6	293 $\pm$ 52*	315 $\pm$ 27*	326 $\pm$ 35*
<b>ATPase activity (nmol Pi mg protein<sup>-1</sup> min<sup>-1</sup>) in PMVs purified from leaves</b>				
	<b>n</b>	<b>CB</b>	<b>CD</b>	<b>PH</b>
Control	18	597 $\pm$ 61		
1 $\mu$ M	8	588 $\pm$ 104	589 $\pm$ 39	585 $\pm$ 15
10 $\mu$ M	6	531 $\pm$ 57	570 $\pm$ 68	642 $\pm$ 105
50 $\mu$ M	6	328 $\pm$ 70*	460 $\pm$ 50*	464 $\pm$ 35*

**Table 1:** Effects of cytochalasin B (CB), cytochalasin D (CD) and phalloidin PH) on proton pumping and vanadate-sensitive ATPase activity of plasma membrane vesicles (PMVs) purified from roots and leaves of *Beta vulgaris*. n: number of measurements from three independent PMV preparations. Mean  $\pm$  SD. \*, significantly different from the control at P = 0.95 with the Student-Fisher *t* test.

<b>Proton pumping (OD units mg protein<sup>-1</sup> min<sup>-1</sup>) in PMVs purified from roots</b>				
	<b>n</b>	<b>CB</b>	<b>CD</b>	<b>PH</b>
Control	12	0.576 $\pm$ 0.088		
1 $\mu$ M	6	0.600 $\pm$ 0.087	0.568 $\pm$ 0.032	0.552 $\pm$ 0.088
10 $\mu$ M	6	0.552 $\pm$ 0.024	0.560 $\pm$ 0.072	0.554 $\pm$ 0.104
50 $\mu$ M	6	0.408 $\pm$ 0.024*	0.410 $\pm$ 0.080*	0.240 $\pm$ 0.016*
<b>Proton pumping (OD units mg protein<sup>-1</sup> min<sup>-1</sup>) in PMVs purified from leaves</b>				
	<b>n</b>	<b>CB</b>	<b>CD</b>	<b>PH</b>
Control	12	0.373 $\pm$ 0.020		
1 $\mu$ M	6	0.377 $\pm$ 0.024	0.342 $\pm$ 0.008	0.334 $\pm$ 0.061
10 $\mu$ M	6	0.360 $\pm$ 0.023	0.390 $\pm$ 0.060	0.412 $\pm$ 0.043
50 $\mu$ M	6	0.260 $\pm$ 0.024*	0.277 $\pm$ 0.080*	0.282 $\pm$ 0.022*
<b>ATPase activity (nmol Pi mg protein<sup>-1</sup> min<sup>-1</sup>) in PMVs purified from roots</b>				
	<b>n</b>	<b>CB</b>	<b>CD</b>	<b>PH</b>
Control	12	391 $\pm$ 56		
1 $\mu$ M	8	437 $\pm$ 55	467 $\pm$ 96	425 $\pm$ 62
10 $\mu$ M	6	430 $\pm$ 30	405 $\pm$ 30	401 $\pm$ 36
50 $\mu$ M	6	293 $\pm$ 52*	315 $\pm$ 27*	326 $\pm$ 35*
<b>ATPase activity (nmol Pi mg protein<sup>-1</sup> min<sup>-1</sup>) in PMVs purified from leaves</b>				
	<b>n</b>	<b>CB</b>	<b>CD</b>	<b>PH</b>
Control	18	597 $\pm$ 61		
1 $\mu$ M	8	588 $\pm$ 104	589 $\pm$ 39	585 $\pm$ 15
10 $\mu$ M	6	531 $\pm$ 57	570 $\pm$ 68	642 $\pm$ 105
50 $\mu$ M	6	328 $\pm$ 70*	460 $\pm$ 50*	464 $\pm$ 35*

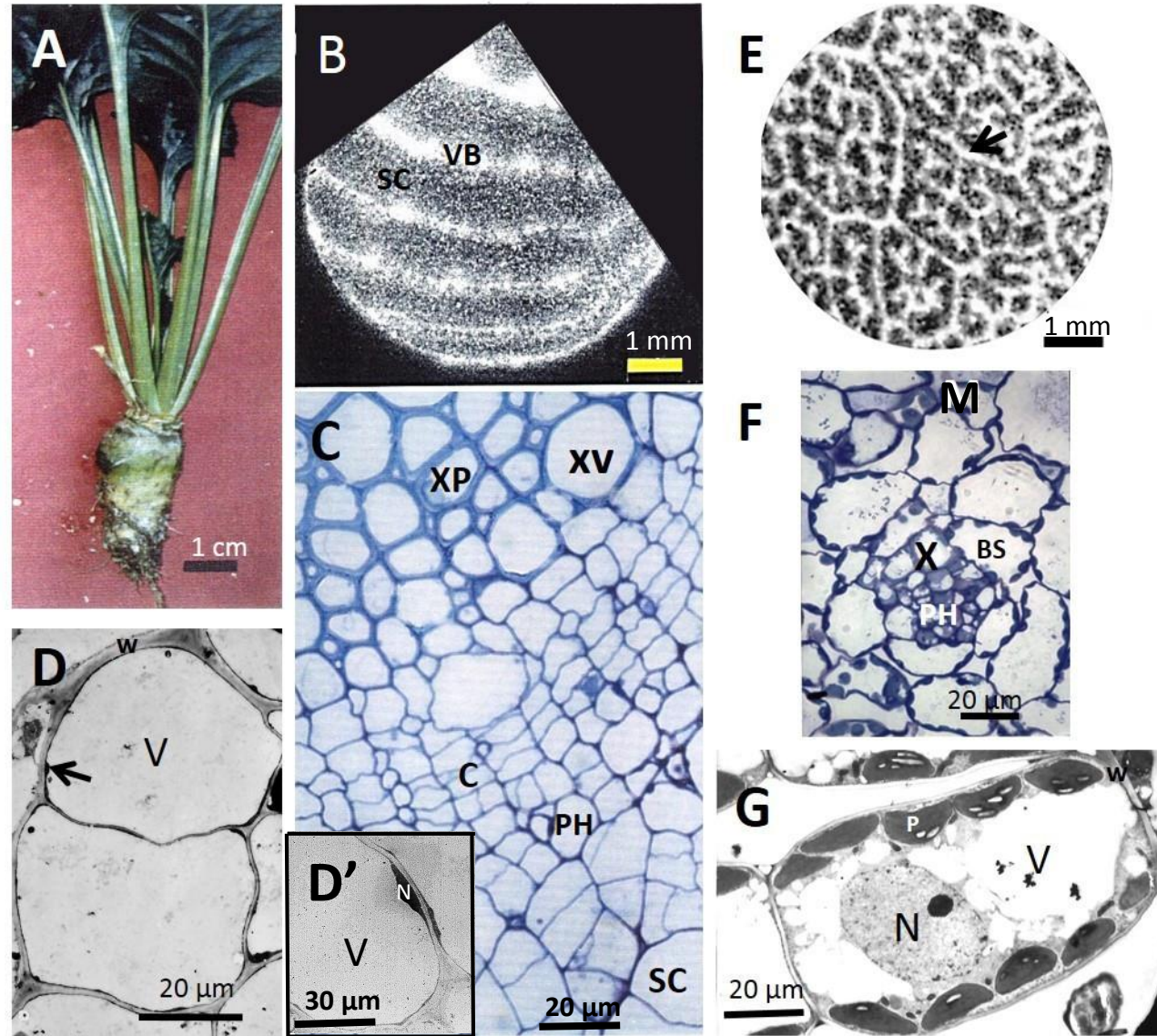
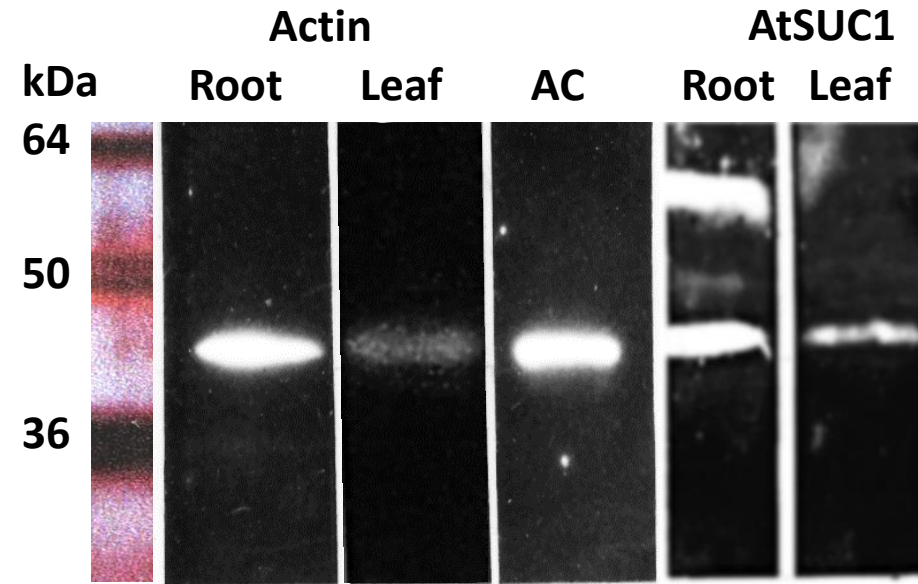


Figure 1

1  
2  
3  
4  
5  
6  
7  
8  
9  
10  
11  
12  
13  
14  
15  
16  
17  
18  
19  
20  
21  
22  
23  
24  
25  
26  
27  
28  
29  
30  
31  
32  
33  
34  
35  
36  
37  
38  
39  
40  
41

Figure 2



1  
2  
3  
4  
5  
6  
7  
8  
9  
10  
11  
12  
13  
14  
15  
16  
17  
18  
19  
20  
21  
22  
23  
24  
25  
26  
27  
28  
29  
30  
31  
32  
33  
34  
35  
36  
37  
38  
39  
40  
41

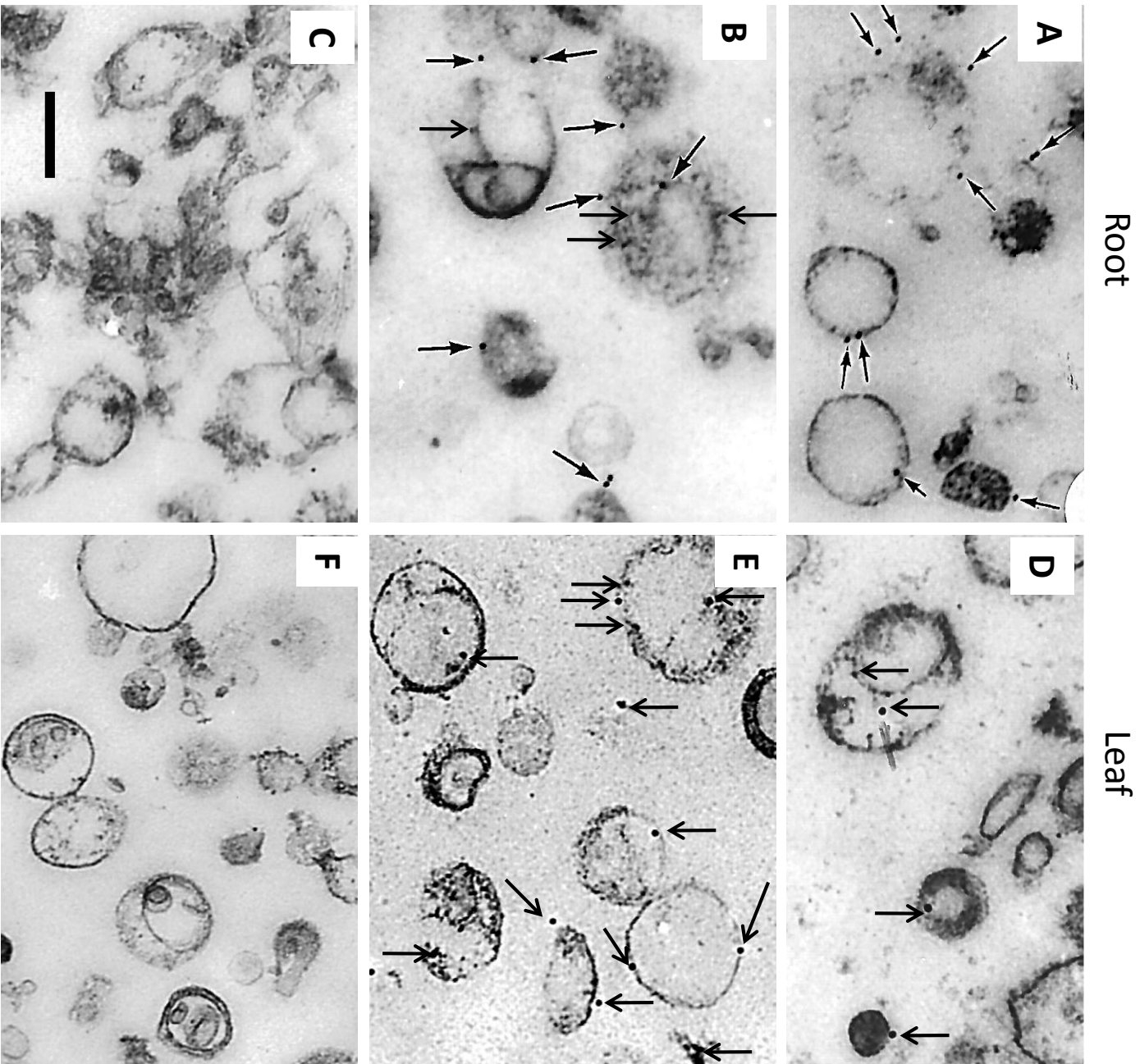


Figure 3

Root

Leaf

C

B

A

F

E

D

1  
2  
3  
4  
5  
6  
7  
8  
9  
10  
11  
12  
13  
14  
15  
16  
17  
18  
19  
20  
21  
22  
23  
24  
25  
26  
27  
28  
29  
30  
31  
32  
33  
34  
35  
36  
37  
38  
39  
40  
41

Figure 4

1  
2  
3  
4  
5  
6  
7  
8  
9  
10  
11  
12  
13  
14  
15  
16  
17  
18  
19  
20  
21  
22  
23  
24  
25  
26  
27  
28  
29  
30  
31  
32  
33  
34  
35  
36  
37  
38  
39  
40  
41

ROOT

LEAF

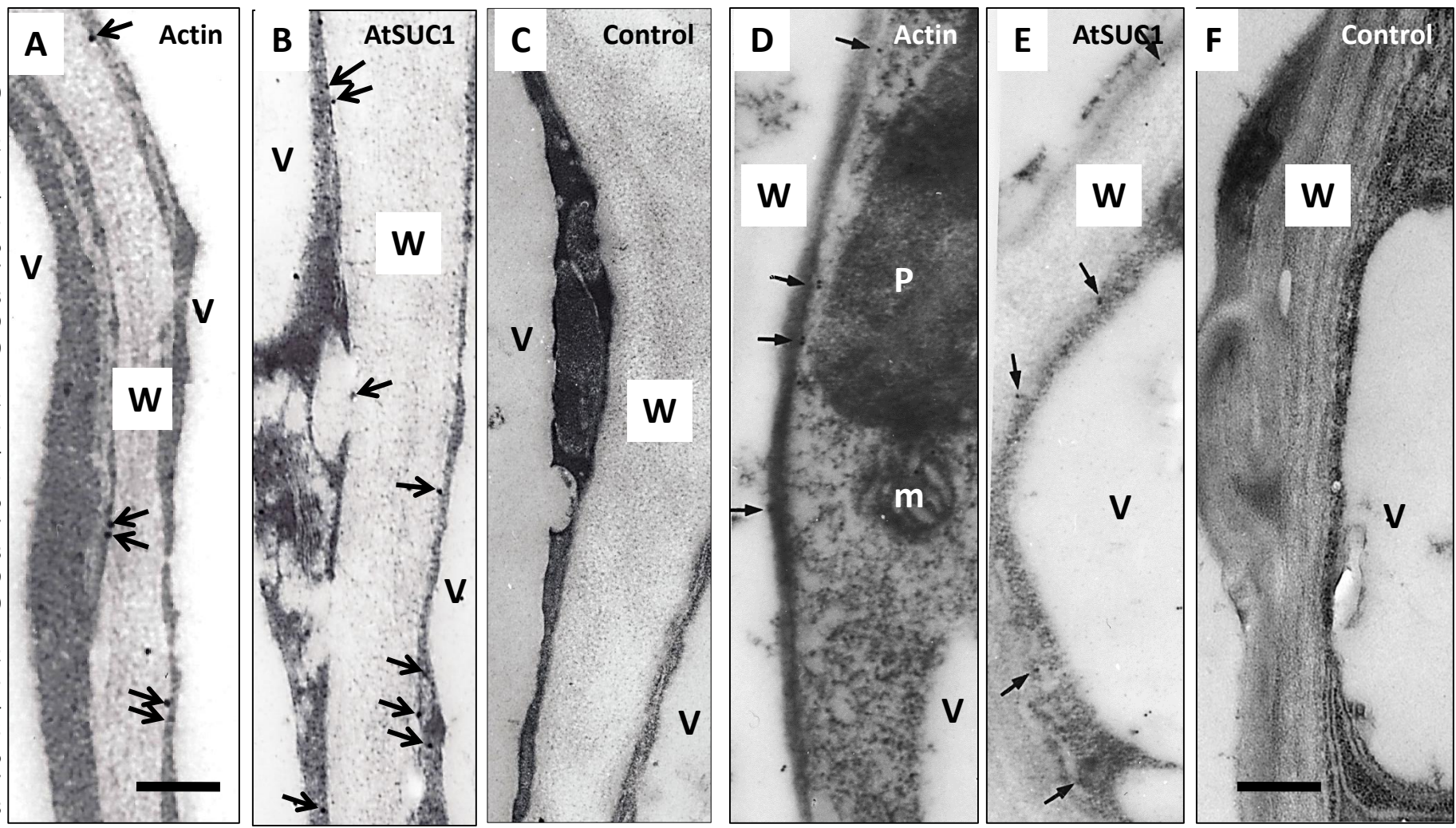


Figure 5

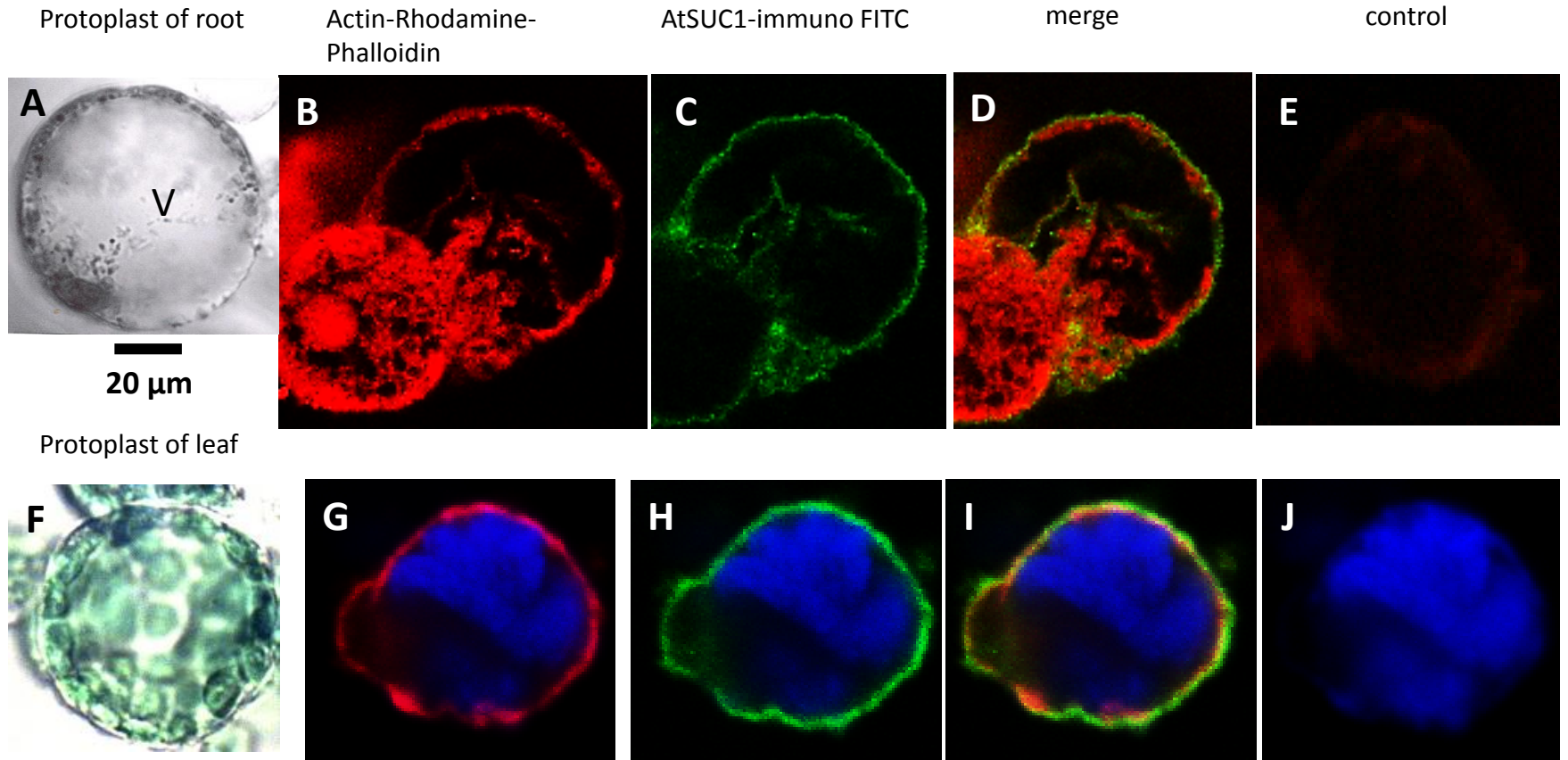
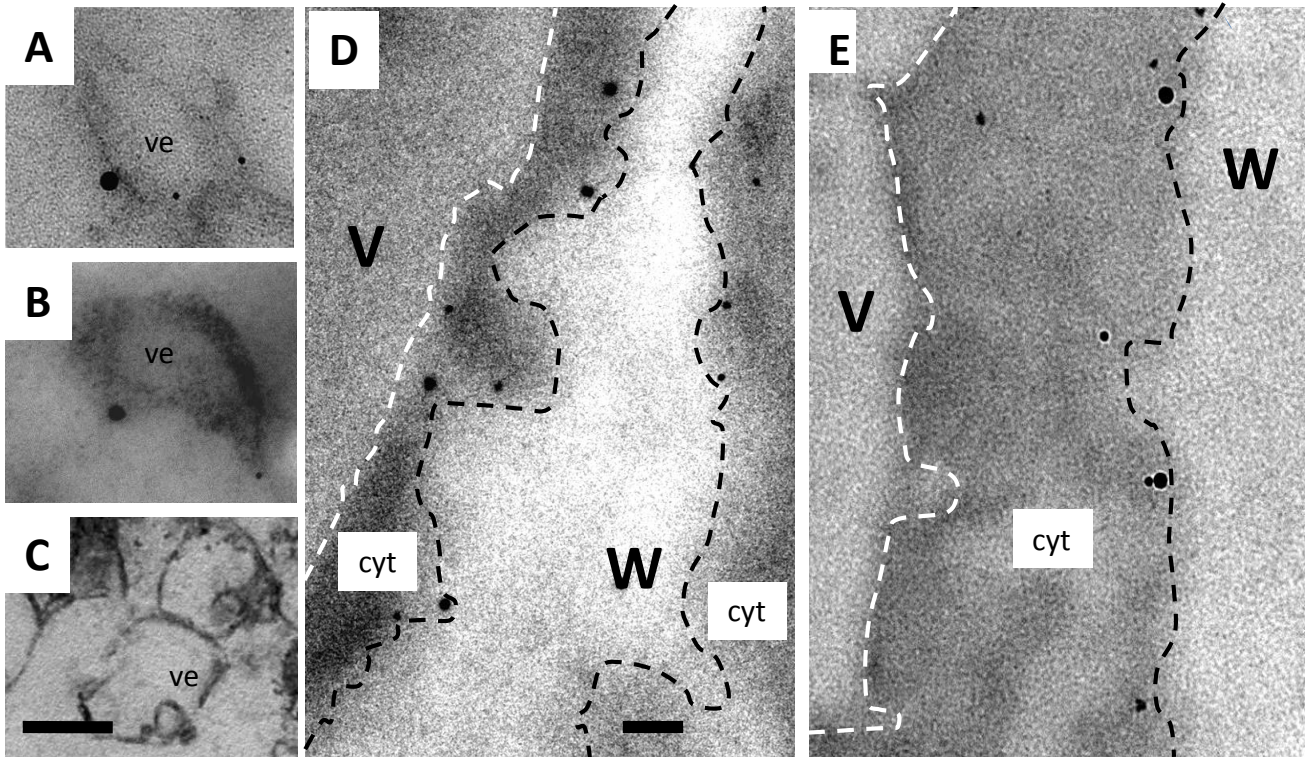
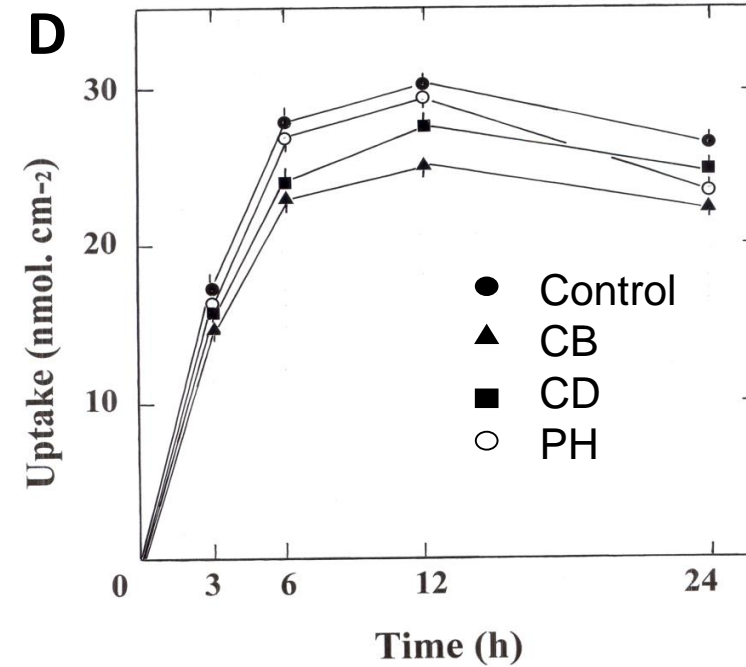
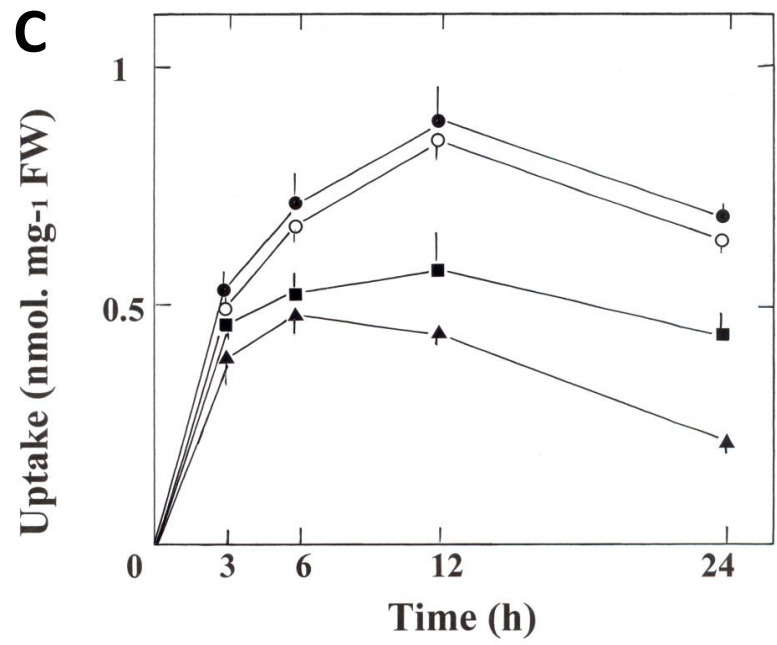
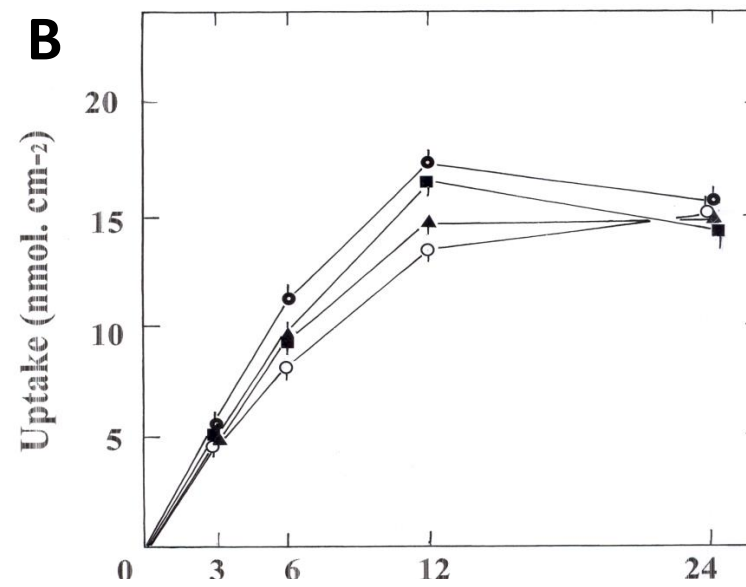
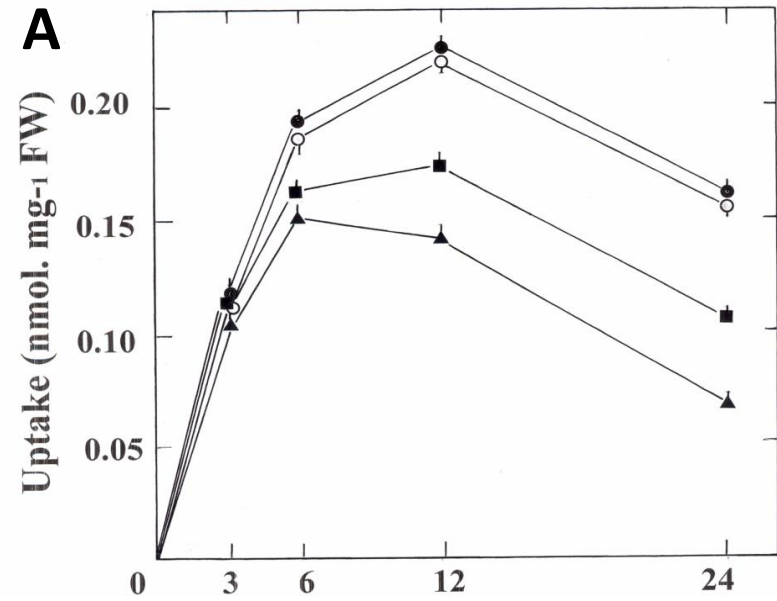


Figure 6



1  
2  
3  
4  
5  
6  
7  
8  
9  
10  
11  
12  
13  
14  
15  
16  
17  
18  
19  
20  
21  
22  
23  
24  
25  
26  
27  
28  
29  
30  
31  
32  
33  
34  
35  
36  
37  
38  
39  
40  
41

Figure 7



1  
2  
3  
4  
5  
6  
7  
8  
9  
10  
11  
12  
13  
14  
15  
16  
17  
18  
19  
20  
21  
22  
23  
24  
25  
26  
27  
28  
29  
30  
31  
32  
33  
34  
35  
36  
37  
38  
39  
40  
41

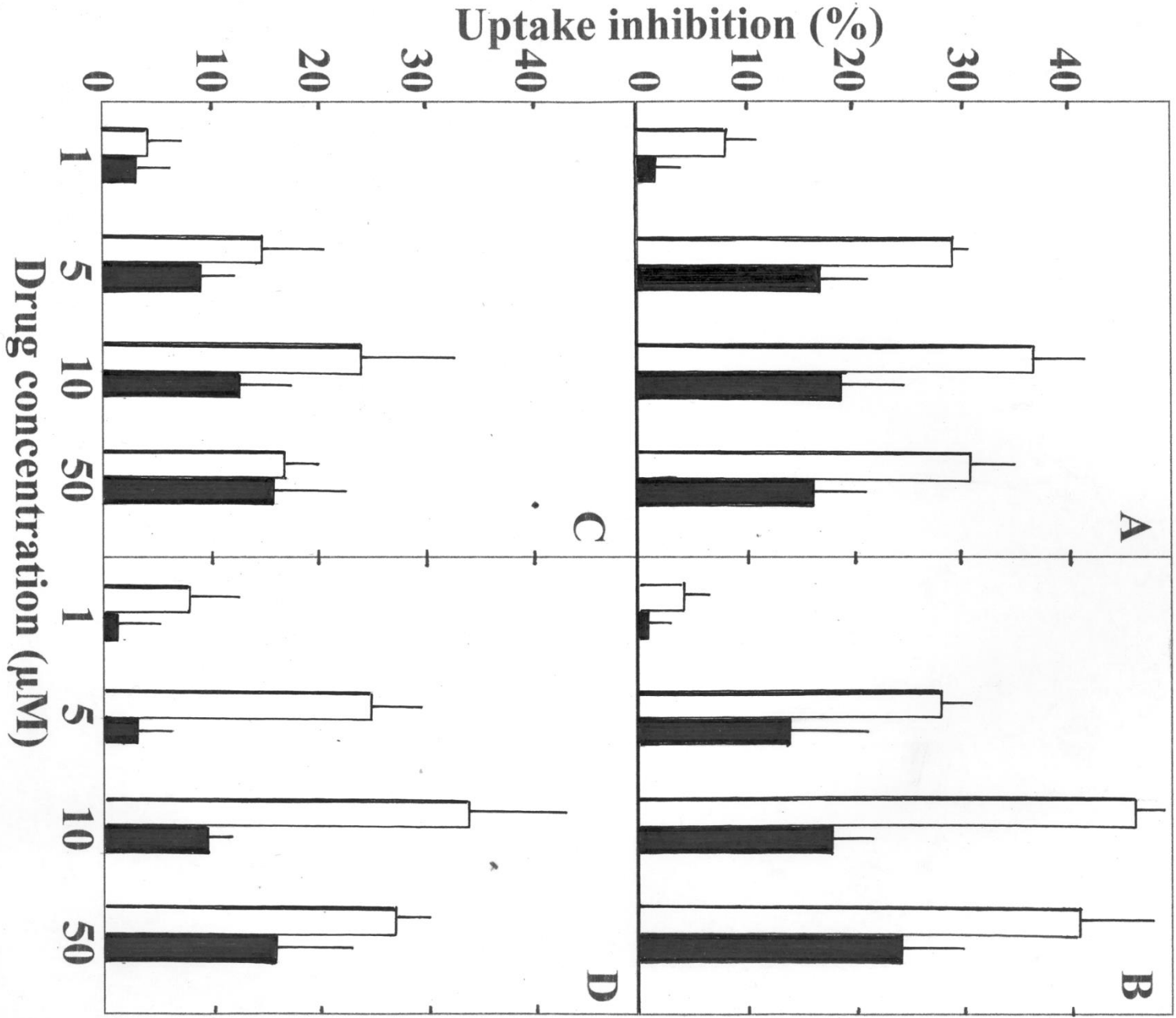
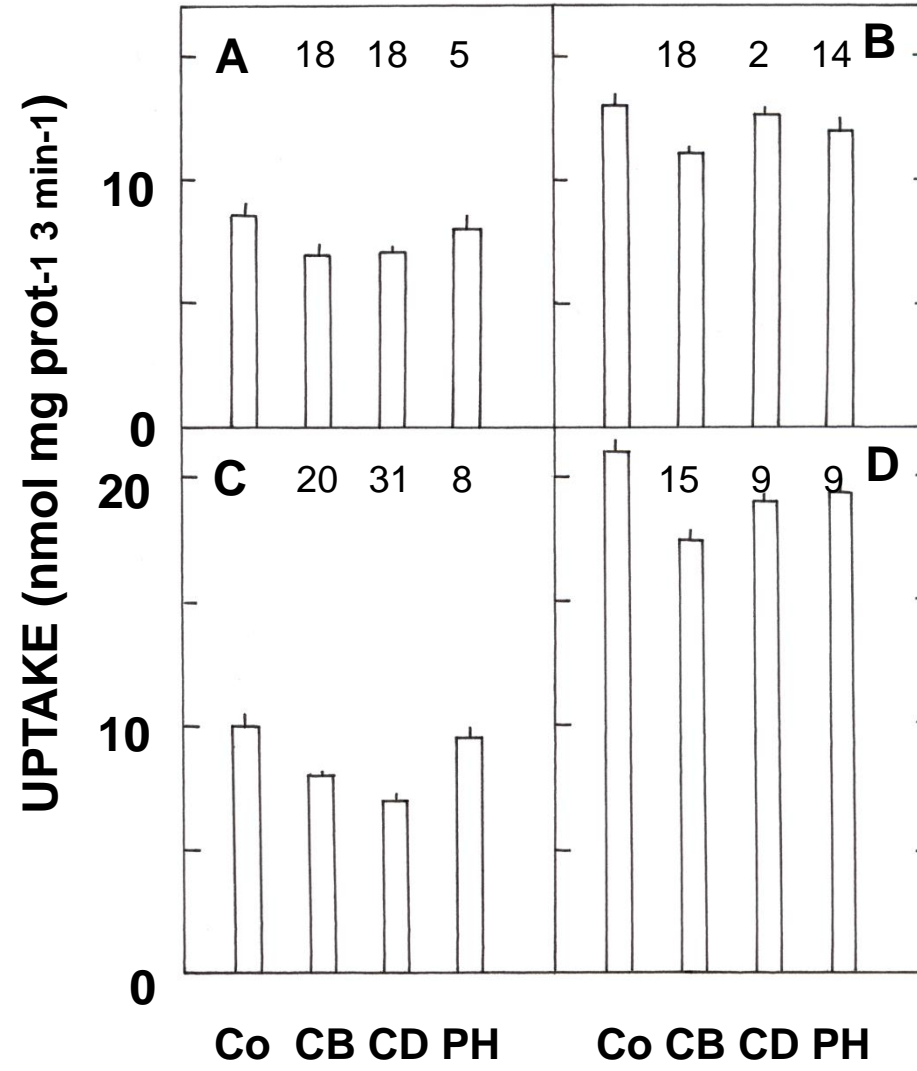


Figure 8

1  
2  
3  
4  
5  
6  
7  
8  
9  
10  
11  
12  
13  
14  
15  
16  
17  
18  
19  
20  
21  
22  
23  
24  
25  
26  
27  
28  
29  
30  
31  
32  
33  
34  
35  
36  
37  
38  
39  
40  
41

Figure 9



1  
2  
3  
4  
5  
6  
7  
8  
9  
10  
11  
12  
13  
14  
15  
16  
17  
18  
19  
20  
21  
22  
23  
24  
25  
26  
27  
28  
29  
30  
31  
32  
33  
34  
35  
36  
37  
38  
39  
40  
41